

## THE FREQUENCY SELECTIVITY OF AUDITORY NERVE FIBRES AND HAIR CELLS IN THE COCHLEA OF THE TURTLE

BY A. C. CRAWFORD AND R. FETTIPLACE

*From the Physiological Laboratory, University of Cambridge,  
Downing Street, Cambridge*

(Received 16 August 1979)

### SUMMARY

1. The electrical responses of single auditory nerve fibres or cochlear hair cells were recorded in the isolated half-head of the turtle *Pseudemys scripta elegans*. Responses to sound stimuli presented to the tympanum could be recorded for at least 4 hr after isolation.

2. Impulses were recorded extracellularly from single auditory nerve fibres. For tones of suprathreshold intensity the impulses occurred with a preferred phase relation (i.e. they were phase-locked) to the cycles of the sound stimulus. Nerve fibres had sharp tuning curves ( $Q_{10\text{ dB}} = 0.5\text{--}7.5$ ) with single characteristic frequencies (c.f.) ranging from about 30 to 700 Hz. Best threshold sensitivities of fibres at their c.f. were in the region of 30–40 db sound pressure level with respect to 20  $\mu\text{Pa}$ .

3. Intracellular recordings were made from hair cells in the basilar papilla. Following injection of a fluorescent dye into a cell through the recording electrode, the dye was localized in a single hair cell in a transverse section of the cochlea.

4. Hair cells had resting potentials of about  $-50\text{ mV}$ , and, to low frequency tones, gave periodic responses graded with the intensity and frequency of the stimulus. Recordings were obtained from cells with characteristic frequencies between 70 and 670 Hz.

5. The voltage response to a pure tone at low sound pressure was sinusoidal for all frequencies of stimulation; at higher sound pressures a number of non-linearities were apparent in the response wave form. One of these was a steady depolarizing component, which, relative to the periodic component of the response, was most prominent at high frequencies.

6. The amplitude of the response evoked in a hair cell by a low intensity tone was linearly related to the sound pressure; for loud sounds, the response eventually reached a saturating amplitude, which in some cells was as great as 30–45 mV peak-to-peak.

7. The linear sensitivity of a hair cell is defined as the r.m.s. voltage for a linear response of the cell at its c.f. divided by the sound pressure at the tympanum. In the most sensitive cells this value was 30–90 mV/Pa.

8. If the frequency selectivity of a hair cell was expressed in terms of the sound pressure needed to produce a constant amplitude of response, the sharpness of this frequency selectivity was found to be virtually independent of the response criterion for responses between 1 and 10 mV; in the cells which gave the largest responses, the

frequency selectivity expressed in this way was comparable to that of the nerve fibres. Cells with smaller maximum responses often had broader tuning curves.

9. Responses of hair cells to short low intensity tone bursts at the c.f. built up approximately exponentially during the tone, and decayed away exponentially when the tone was terminated. The terminal oscillations were at the c.f. of the cell, and independent of the frequency of stimulation.

10. From the time constant of the build up and decay of the linear response to a tone burst at the c.f. the sharpness of tuning of the cell was estimated and found to agree with that obtained from the responses of the cell to continuous tones. The most highly tuned cells had quality factors ( $Q_{3\text{dB}}$ ) in the range 5–10.

11. The c.f. of a hair cell was correlated with its position along the basilar membrane. Low frequency hair cells were located towards the apical or lagenar end and high frequency cells were found towards the basal or saccular end. On the assumption of an exponential distribution of c.f. with distance, each octave occupied about 94  $\mu\text{m}$  along the membrane.

12. A hair cell's response to a click was a decaying oscillation at the characteristic frequency of the cell. From the initial polarity of the responses to condensation and rarefaction clicks it was concluded that the hair cell depolarized as a result of movements of the basilar membrane towards the scala vestibuli, and hyperpolarized for motion towards the scala tympani.

13. In the absence of deliberate sound stimulation, the hair cell voltage fluctuated continuously about its mean level. The principal frequency components in the noise were concentrated around the c.f. of the cell. The voltage noise in the hair cells showed no significant cross-correlation with sound pressure fluctuations at the tympanum.

#### INTRODUCTION

It is generally assumed that the cochlear hair cells are responsible for converting basilar membrane motion into electrical signals which are then relayed via the auditory nerve to the brain. Although the responses of single auditory nerve fibres have been extensively studied (for reviews see Kiang, Watanabe, Thomas & Clark, 1965; Rose, 1970; Evans, 1975) little is known about the functioning of the hair cells and their contribution in shaping the discharge of the nerve fibres. The object of the present work was to examine, by means of intracellular recording, the properties of the hair cells in the cochlea of the turtle *Pseudemys scripta elegans*.

As a measure of the auditory receptor potential, the cochlear microphonic that can be recorded with extracellular electrodes (Adrian, 1931; Dallos, 1973) is unsatisfactory, since at best it probably represents the activity of a large number of cells. However, it has proved difficult to make intracellular recordings from single cochlear hair cells in intact anaesthetized animals. Responses have been reported for these cells in the alligator lizard (Mulroy, Altmann, Weiss & Peake, 1974) and the guinea-pig (Russell & Sellick, 1978). We have tried to avoid the problem inherent in experiments on whole animals by using an isolated reptilian preparation. This type of preparation was originally described by Adrian, Craik & Sturdy (1938) and it offers the advantage of the greater mechanical stability which is needed for intracellular recording.

In this paper our concern has been with describing some of the general properties of the hair cell's responses to pure tones, and assessing to what extent these responses are consistent with the discharge in the auditory nerve fibres. The selectivity of the response for tones of different frequencies has been measured and under the best circumstances is shown to be comparable to the tuning of the nerve fibres in the same kind of preparation. We have suggested previously that the cochlea's frequency selectivity in this animal arises in two stages and that the second stage may reside in the cell itself (Crawford & Fettiplace, 1978; Fettiplace & Crawford, 1978). In a later paper (Crawford & Fettiplace, 1980) we will examine the evidence for this idea in more detail and show that the second filtering stage, which is the most important, may be attributable to an electrical resonance in the hair cell.

#### METHODS

##### *Preparation*

Experiments were performed on the isolated half-head of the red-eared turtle, *Pseudemys scripta elegans*. In most cases juvenile specimens, carapace length 30–35 mm, were used. After decapitation and sagittal sectioning of the head, most of the brain was removed except for a small piece of the medulla which was left attached to the intact auditory and facial nerves. Care was taken to cut the other caudal cranial nerves close to the brain surface and not interfere with the meninges or the periotic sac in the region of the vagal foramen (Adrian *et al.* 1938). The otic capsule was then opened on the cranial side, thus exposing the scala tympani and giving access to the basilar membrane over most of its length, and also to the cochlear ganglion and the neural limb. The half-head was placed in a closed chamber gassed with a moist 95% O<sub>2</sub>:5% CO<sub>2</sub> mixture, as shown in Fig. 1A. The scala tympani was flushed periodically with Ringers solution, the fluid level being maintained close to normal. The composition of the Ringer solution was (Dessauer, 1970): 130 mM-NaCl; 4 mM-KCl; 2.8 mM-CaCl<sub>2</sub>; 2.2 mM-MgCl<sub>2</sub>; 5.0 mM-Tris chloride buffer, pH 7.8. The experimental chamber was positioned on a large steel table mounted on inflated rubber inner tubes which served to isolate the preparation from mechanical vibrations transmitted through the building. The resonant frequency of the table perpendicular to the tympanum was 5.6 Hz as measured with a Brüel & Kjær 8603 accelerometer. In the auditory range, the principal disturbing displacements of the chamber perpendicular to the tympanum were at 98, 242 and 484 Hz and had a maximum amplitude of less than 0.1 nm. Since this is comparable to the displacement of the tympanum at the auditory threshold of the turtle (0.1 nm at 40 db re 20 Pa from the data of Moffat & Capranica, 1978), it seems unlikely that the cochlea is subject to vibrational stimulation in our experiments. Experiments were carried out at room temperature (19–25 °C) and usually lasted for 3–4 hr, over which period there was no evidence of a deterioration in the preparation.

##### *Anatomy*

The anatomy of the labyrinth in *Pseudemys* has been described in detail by Baird (1960, 1974). The anatomy of the cochlea shows considerable variation among different reptiles (Wever, 1978), and the following is a brief summary of the main features of the cochlea in *Pseudemys*. Some of these features are visible in Pl. 1 and Fig. 1B. Pl. 1 shows a photomicrograph of a stained whole-mount of the cochlear duct of a juvenile; Fig. 1B is a drawing of a transverse section through the cochlea near its basal end, and shows the basilar papilla, and the arrangement of the scalae. The cochlear duct, which is homologous to the mammalian structure, is an uncoiled tube which terminates blindly as the lagena. The basilar membrane is roughly elliptical, and the dimensions of the major and minor axes are about 700 and 170  $\mu$ m in juvenile specimens (see Pl. 1). The sensory organ is the basilar papilla, which is seated upon the basilar membrane over towards the neural edge (Fig. 1B). The papilla is composed largely of columnar hair cells, and tapers from about twelve hair cells in width at the apical end near the lagena down to about three hair cells in width at the basal end close to the saccule and contains a total of about 1000 hair cells arranged in about 100 rows. The hair cells are unidirectionally oriented with their

kinocilium placed on the side away from the neural limb (Miller, 1978); these are surmounted over the entire length of the papilla by a tectorial membrane, and the hair cell ciliary bundles project upwards into pockets in the under surface of the tectorial membrane (Miller, 1978). The basilar papilla also contains supporting cells and the terminals of the auditory nerve fibres. The nerve fibres leave the papilla and initially run perpendicular to its long axis in a thin sheet known as the neural limb before uniting with other branches to form the auditory nerve (Pl. 1). There is at present no information available about the innervation of the hair cells. Nor is there any evidence to indicate that in the turtle they are morphologically specialized into categories analogous to the mammalian inner and outer hair cells.

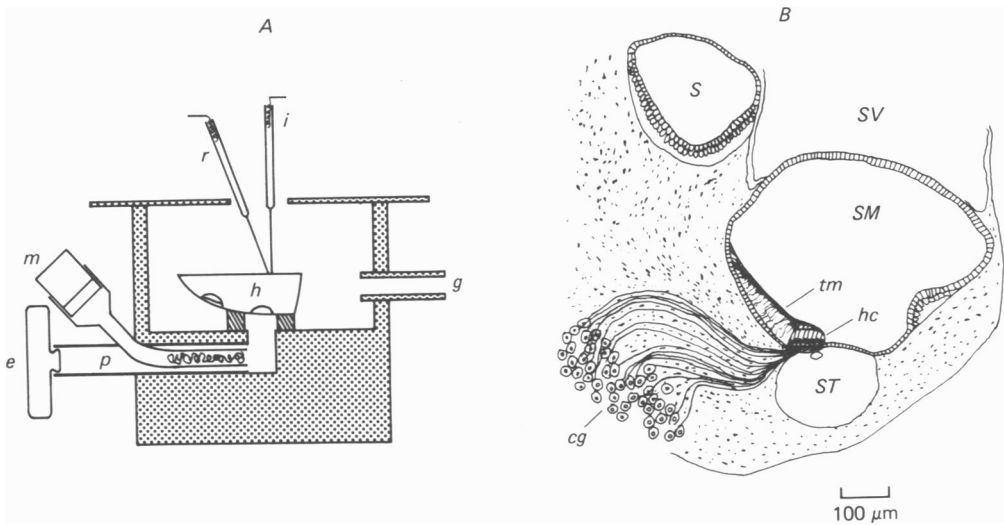


Fig. 1. *A*, diagram of experimental chamber (not drawn to scale). The half-head, *h*, is sealed to the bottom of the chamber with 'Blutak', with the tympanum facing down towards the sound source. Sound was generated with a dynamic earphone, *e*, and the sound pressure near the tympanum was monitored with a  $\frac{1}{4}$  in. (1.27 cm) condenser microphone, *m*, and a critically damped and calibrated probe tube, *p*. The distance from the axis of the probe tube to the tympanum is approximately 5 mm. *i*, intracellular microelectrode; *r*, reference electrode; *g*, inlet tube for moist  $O_2/CO_2$  mixture; space around head packed with moist Kleenex. *B*, drawing of a transverse section of a cochlea fixed in Susa. The section is taken at a level near the saccular end of the basilar membrane. *S*, saccule; *SV*, scala vestibuli; *SM*, cochlear duct or scala media; *ST* scala tympani; *hc*, hair cells in papilla on the basilar membrane; *tm*, tectorial membrane; *cg*, cochlear ganglion, containing cell bodies of auditory nerve fibres. During an experiment, the scala tympani was opened on the medial surface for introduction of the intracellular electrode.

### Intracellular recordings

The electrodes for recording intracellularly were glass micropipettes drawn from Pyrex Omega dot tubing on a Livingston-type puller (Takahashi Seiki Kogyo Co. Ltd., Tokyo, Japan) and filled by injection with 4 M-potassium acetate. Satisfactory electrodes had resistances, measured in Ringer solution, of 250–500 M $\Omega$ . The recording electrode was connected to a high input impedance preamplifier with capacity compensation which was based on the design of Colburn & Schwartz (1972). This amplifier also had the facility for injecting a constant current through the recording electrode and balancing out the voltage developed in the electrode resistance. The magnitude of the injected current was calculated from the voltage drop across the feed-back resistance  $R_s$  (see Colburn & Schwartz, 1972) which was 100 M $\Omega$ . The input current of the amplifier which was limited by the current injection circuit, was adjusted to be about 1 pA maximum. In all experiments the reference electrode was a Ringer bridge placed

on the auditory nerve. The intracellular electrode was introduced into the scala tympani and advanced so that it penetrated the basilar membrane and papilla from the perilymphatic surface. When the electrode was in the papilla, capacity compensation was applied so as to square up as well as possible the initial phase of the voltage response to a small injected current step. An attempt was made to estimate the frequency response of the recording system by passing a 0.1 nA sinusoidal current down the electrode. This was done with the electrode placed just

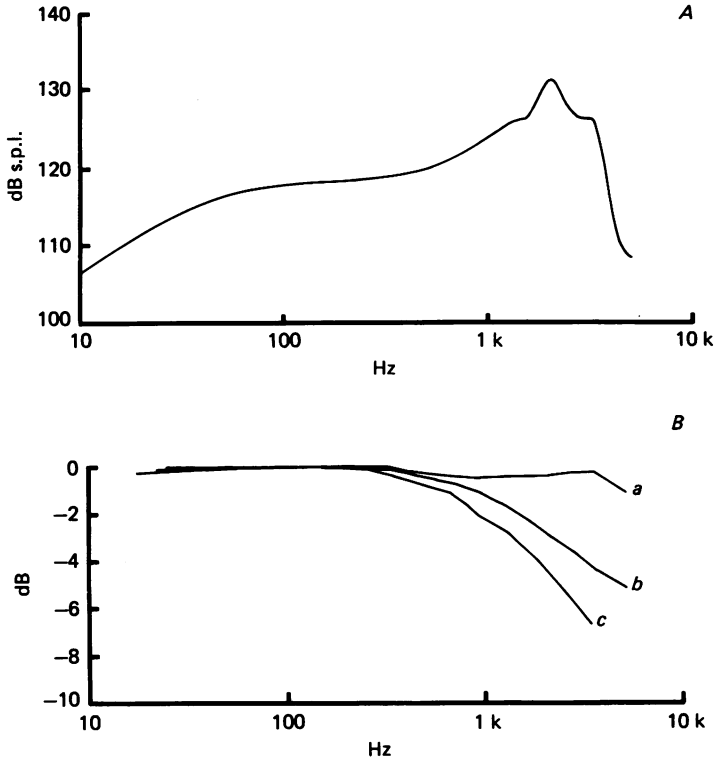


Fig. 2. *A*, frequency response of the unattenuated sound delivery system for a constant voltage input to the earphone, swept from 10 Hz to 5 kHz. The sound pressure at the tympanum, plotted on the ordinate in decibels re 20  $\mu$ Pa was measured through a calibrated probe tube. The probe tube correction is not included, but was less than  $\pm 1$  db below 1 kHz. The sound level varied over about 5 db from 100 Hz to 1 kHz. In each experiment a sound calibration curve of the type shown was measured (DT 505 earphone). *B*, frequency response of the recording system in three different experiments. These were obtained with the intracellular electrode just outside a cell by injecting a 0.1 nA sinusoidal current, whose frequency was swept from about 15 Hz to 5 kHz. The attenuation of the voltage relative to that at low frequency is plotted on the ordinate in decibels. The low frequency resistance of the intracellular electrode was: *a*, 355  $M\Omega$ ; *b*, 340  $M\Omega$ ; *c*, 585  $M\Omega$ .

outside a cell, before or after an experiment. Examples of the frequency response of the recording system for three different electrodes are shown in Fig. 2*B*. The fastest recording system was obtained if the fluid level in the scala tympani was low (less than 200  $\mu$ m) so as to minimize the uncompensatable distributed capacitance in the electrode. On average, however, the recording system had a 3db bandwidth of about 3 KHz, which corresponds to a stray capacity of 0.1–0.2 pF. For a variety of reasons it is likely that the electrode resistance may be higher when the electrode tip is inside the cell (see e.g. Eisenberg & Johnson (1970), p. 51). Our estimates of the bandwidth of the recording system thus provide only an upper limit, and the periodic component

of the hair cell potentials above 1 kHz may have been subject to some attenuation. All data during an experiment was recorded at 15 in./sec on an FM tape recorder (Racal Store 4) with a band width DC to 5 kHz.

Penetration of cells was accomplished by applying an oscillating voltage to the electrode tip by over-compensating the capacitance neutralization (see Baylor, Fuortes & O'Bryan, 1971). This could be achieved without disturbing the setting previously established for neutralizing the input capacity. Intracellular recordings were made from more than sixty hair cells, with maximum peak-to-peak responses of 10 mV or more; however, most of the information in the results is derived from twenty-three of these cells, each of which gave a maximum response of over 15 mV. The mean duration of a recording was about 20 min, but several cells were held for up to an hour.

The high resistance of the intracellular micro-electrode introduced considerable noise into the electrical records, in addition to any biological noise present, which could also be substantial (see Results). Thus in order to improve the resolution in the recordings of responses to tone bursts, these responses were often subsequently averaged on a Biomac 500 signal averaging computer. To achieve a signal-to-noise improvement in the responses to tones of swept frequency these responses were measured with two phase-lock amplifiers (Brookdeal 9503 SC and 5042 omniphase). The amplifiers were referenced in quadrature to the driving signal delivered to the earphone and were set in the 'sinetrac' mode in order to measure the amplitude and phase of the fundamental component of the hair cell's response. This technique was used to obtain the linear iso-intensity tuning curve of a hair cell, the measuring band width being 0.25–2.5 Hz.

Noise spectra were measured with the two phase-lock amplifiers on pieces of record about 30–60 sec in duration. Spot measurements were made at a series of frequencies determined by that of an external reference signal supplied from an independent oscillator. The time constant  $T$  of the phase-lock loop was set at 300 msec, and hence the noise equivalent band width  $\frac{1}{4}T$  (see Gardner, 1966) was 0.833 Hz. The modulus output of the 'omniphase' was smoothed with a 6 sec time constant. The method was used for obtaining spectra of the noise in the voltage recordings and also the spectrum of the room noise.

#### *Extracellular recordings*

Impulses were recorded extracellularly from auditory nerve fibres using glass micropipettes filled with 3 M-NaCl (resistances in Ringer solution 20–40 M $\Omega$ ). The impulses were amplified and displayed on an oscilloscope, or fed into earphones for audiovisual determination of the threshold response. This was accomplished by adjusting the sound stimulus until it was just possible to see or hear a change in the pattern of the impulse discharge above the spontaneous level. In some experiments, peri-stimulus histograms of the timing of the impulses were constructed using the Biomac. The audiovisual threshold corresponded approximately to a doubling in the firing rate over the spontaneous level on the peaks of the responses.

The extracellular recordings were obtained with the electrode either in the auditory nerve or, in three experiments, in the neural limb adjacent to the papilla. In all cases, the scala tympani had been opened and the preparation was identical to that used for intracellular recordings from cells in the papilla. When recordings were made in the eighth nerve, units were sometimes obtained which were not driven by auditory stimuli. Some of these had rhythmic activity which could be altered by rocking the anti-vibration table on which the preparation was mounted.

#### *Dye marking of hair cells*

When the intracellular micro-electrode was in a cell in the basilar papilla one of two categories of response to sound could be recorded, and these were distinguishable as described in the Results. In order to verify which response was originating in the hair cells, we carried out a series of experiments to mark the impaled cell by injecting a fluorescent dye, Lucifer yellow CH (Stewart, 1978) from the electrode. The electrodes were filled with a 5% solution of the Li salt of the dye and had resistances of 1–2 G $\Omega$ . The dye was ionophoresed into cells by 0.5 sec pulses of inward current (0.5–1.0 nA). The response of the cell to sound was checked periodically during the current injection and the process terminated if the response failed. After an experiment, the half-head was fixed in 4% formaldehyde buffered with 0.1 M-phosphate, pH 7.2. The cochlea was subsequently dissected out, embedded in paraffin wax and cut into transverse sections 10  $\mu$ m in thickness.

Dye-marked cells were localized in the sections by their yellow-green fluorescence. Out of twenty-two cells which were injected, seven hair cells were clearly stained and no dye was found in any other type of cell. An example of a section containing a dye marked hair cell is shown in Pl. 2.

### *Sound stimulation*

Tones were generated by a dynamic earphone (Beyer DT505 or DT48) connected to the ear via a sealed coupler (see Fig. 1). The sound pressure near the tympanum expressed in the text in decibels sound pressure level (db s.p.l.) relative to  $20 \mu\text{Pa}$  ( $\text{Pa} = \text{N/m}^2$ ), was monitored with a calibrated  $\frac{1}{2}$  in. (1.27 cm) condenser microphone (Brüel & Kjaer, 4134) and probe tube. The microphone was connected through its preamplifier to a measuring amplifier (Brüel & Kjaer, 2608). The probe tube was damped and calibrated, either separately using a Brüel & Kjaer coupler or in the experimental chamber by substituting a second microphone in the position of the tympanum. An example of the frequency response of the sound-producing system under experimental conditions is shown in Fig. 2A.

For producing tone bursts or clicks, the driving sinusoid delivered to the earphone was generated by gating the output of a function generator (Feedback TWG 500). The sinusoid was gated at a fixed point in the cycle, thus ensuring that the phase of the sinusoid and the number of cycles within a tone burst were the same for each of a given set of stimuli. The output of the function generator was then attenuated by a Hatfield 2135 balanced attenuator and fed through a driver amplifier to the earphone. Tone bursts were sometimes shaped by bandpass filtering prior to attenuation. This was done using six-pole Butterworth high and low-pass filters set as close to the stimulating frequency as possible. This arrangement also had the virtue of reducing the harmonic distortion in the output of the function generator.

Swept-frequency continuous tones were generated by a digital oscillator. This operated by reading cyclically through a quarter cycle sine table in a read-only memory (Signetics, 256 by 8 bit ROM programmed by Farnell). The resulting sine wave contained 1024 points per cycle, and its frequency could be varied continuously depending upon the rate at which the numbers in the table were transferred. This was determined by a clock whose frequency was controlled, up to a maximum of 10 MHz, by a ramp voltage. For most experiments the frequency of the output signal was swept exponentially from 5 Hz to 5 kHz over a duration of about 1 min. Since the full range of the signal was quantized into 512 levels, there was an error in the sine wave which was equivalent to an added noise. It may be shown (Bendat & Piersol, 1971, p. 232) that the signal-to-noise ratio is about 60 db.

For swept tones and filtered tone bursts of frequencies above 30 Hz the second harmonic in the sound stimulus was less than  $-62$  db relative to the fundamental when the sound pressure of the fundamental was at 120 db s.p.l. The second harmonic was the major distortion product in the sound and, under these conditions, was generated chiefly by the earphone. For unfiltered tone bursts, the second harmonic distortion was determined by the function generator and was less than  $-48$  db relative to the fundamental.

No precautions were taken to sound-proof the preparation, this being originally justified in terms of the lower auditory sensitivity of the turtle as compared to the mammal. On several occasions, however, the background noise in the room was measured, and was found to have a total pressure of about 56 db s.p.l. at the tympanum in the frequency band 5 Hz–5 kHz. The spectrum of the noise was pink, i.e. its amplitude fell linearly with frequency and had a value of the order of  $3 \times 10^{-4}$  Pa/ $\sqrt{\text{Hz}}$  at 100 Hz.

### *Correlation measurements*

Cross-correlation functions between pressure and voltage ( $R_{pV}$ ) were calculated (Bendat & Piersol, 1971) as

$$R_{pV}(\tau) = \frac{1}{T} \int_0^T p(t) \cdot V(t+\tau) dt, \quad (1)$$

where  $p(t)$  and  $V(t)$  are simultaneous samples of duration  $T$ , of the sound pressure fluctuations and the hair cell voltage fluctuations respectively, and  $\tau$  is the lag time. All cross-correlation

functions were normalized to give the cross-correlation coefficient ( $\rho_{pV}$ ) by

$$\rho_{pV}(\tau) = \frac{R_{pV}(\tau)}{\sqrt{\sigma_p^2 \sigma_V^2}}, \quad (2)$$

where  $\sigma_p^2$  and  $\sigma_V^2$  are the variances of the samples of acoustic noise and hair cell voltage noise respectively.  $\rho_{pV}(\tau)$  then lies in the range +1 to -1. Computations were performed on a PDP-11 laboratory computer according to the direct procedure outlined by Bendat & Piersol (1971, p. 332), using a programme written by Dr T. D. Lamb. Sample records varied between 512 and 4096 points with an interpoint interval of 0.5 ms. All samples were low-pass filtered at 700 Hz using a six-pole active filter to prevent aliasing. The standard deviation of the correlation coefficient ( $SD_\rho$ ) is given (Bendat & Piersol, 1971) by

$$SD_\rho = \frac{1}{\sqrt{2BT}} \{1 + \rho^2\}^{\frac{1}{2}}, \quad (3)$$

where  $B$  is the bandwidth of the correlation, in this case 1 kHz. Values of  $SD_\rho$  are given in the text.

Triggered correlation functions between sound pressure at the tympanum and auditory nerve discharge were obtained according to the methods of de Boer (1968). Samples of auditory nerve discharge were obtained both in the absence of intentional acoustic stimulation and under conditions where the preparation was stimulated with noise signals at different levels. Electrical noise signals were produced by a pseudo-random noise generator, clocked through a 65535 sequence at 5 kHz. Triggered correlograms were obtained by using each spike in the nerve discharge, played backwards from the tape recorder, to trigger the sweep of an averaging computer (Biomac 500) and thus averaged 20 ms samples of the sound pressure at the tympanum that preceded each sweep. Between 1024 and 16384 sweeps were collected for each correlogram. The procedure reveals consistent features (if any) of the pressure wave form that immediately precedes the occurrence of a spike in the auditory nerve. If the ear is stimulated with white noise the triggered correlogram under certain conditions is related to the impulse response of the pathway leading to the nerve fibre (de Boer & Kuypers, 1968; de Boer, 1968).

## RESULTS

### *The responses of auditory nerve fibres*

In the first part of the investigation, we were concerned with establishing the capabilities of the cochlea in the isolated preparation, by recording the responses of single fibres in the auditory nerve. The nerve fibres continued to give responses to sound for several hours after beginning an experiment, and there was no major deterioration in sensitivity or sharpness of tuning over this period. The nerve fibres responded to sounds containing frequency components between about 10 Hz and 1 kHz, and the pattern of responses resembled that previously described for low frequency fibres of the mammalian auditory nerve. Some of the properties of the responses are illustrated in Fig. 3, which gives histograms of the probability of firing of a single fibre to tone bursts at its characteristic frequency at various intensities. In the absence of an applied sound, each nerve fibre exhibited a spontaneous discharge of impulses, whose mean rate varied from one fibre to another between a few impulses per sec up to about 70 per sec. In response to pure tones, the impulses synchronized at a constant phase to the cycles of the sound stimulus, and for low intensities the firing was modulated approximately sinusoidally about the basal level, thus reflecting the stimulus wave form. This can be seen for the responses to the lowest intensities for the cell of Fig. 3; the spontaneous firing rate was about 60 spikes/sec and in response to a 165 Hz tone at 40 db s.p.l. (the second lowest in-



tensity not shown in Fig. 3) the firing rate increased to 108 spikes/sec on the peaks and declined well below the spontaneous level in the dips. This response was judged to be a threshold one at that frequency on the basis of the audiovisual criteria that were usually used for defining the threshold (see Methods).

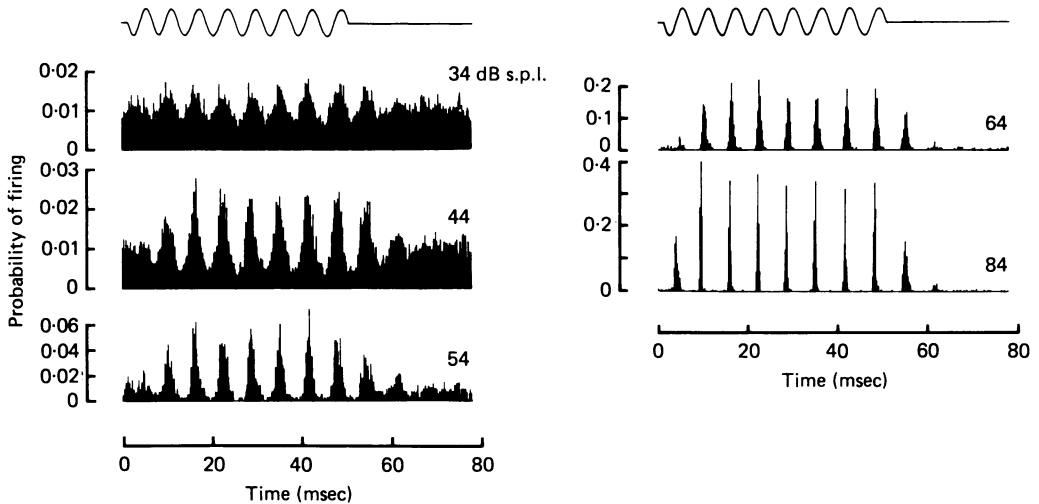


Fig. 3. Responses of an auditory nerve fibre to tone bursts at its characteristic frequency, 165 Hz, at various sound pressures. At each pressure, histograms of the timing of the extracellularly recorded impulses were constructed from between 200 and 2500 stimulus presentations; bin width 0.16 ms. The top trace on left and right is the sound monitor. Number beside each histogram is sound pressure in decibels sound pressure level relative to  $20 \mu\text{Pa}$  (db s.p.l.). 20 db is equivalent to a tenfold change in sound pressure;  $\text{Pa} = \text{N/m}^2$ . A probability of firing of 0.01 corresponds to an instantaneous firing rate of 62.5 spikes/s, which was approximately equal to the spontaneous firing rate in this cell. In this and succeeding figures, the sound monitor is drawn with compressions being positive.

The firing rate on the peaks of the responses increased approximately linearly with sound pressure for low pressures (up to about 65 db s.p.l. in Fig. 3) but then sharply saturated. The range over which the sound pressure could be coded in terms of the firing rate was thus about 30–40 db. In some cells, a marked phasic component appeared at high sound levels at the beginning of the response, and this was accompanied by a transient cessation in firing immediately the tone burst ended. The phasic component became more pronounced at higher frequencies of 1 kHz or more. At 1 kHz there was still evidence in the nerve fibre responses of phase-locking of the impulses to the cycles of the sound.

The frequency selectivity or 'tuning' of a nerve fibre was determined by measuring the sound pressure required to produce a threshold response as a function of frequency. Frequency-threshold curves were determined for 142 fibres in eleven animals. Each fibre responded selectively to a narrow band of sound frequencies, and had a single characteristic frequency (c.f.) at which the threshold sound pressure was a minimum. Different fibres had different c.f.s, but these were distributed evenly and

unimodally in the range 30–700 Hz. There was no evidence of any large gaps or discontinuities in the frequency representation in this range although the accuracy with which this point could be established was limited by the small number of fibres sampled. The continuity is best judged by the results shown in Figs. 5 and 6.

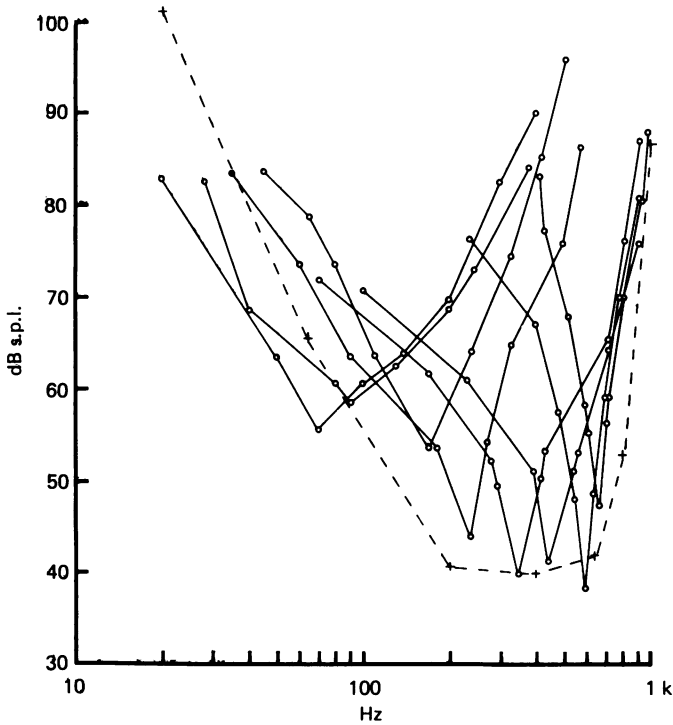


Fig. 4. Frequency–threshold curves for eight representative auditory nerve fibres from one animal. Sound pressure at tympanum required to produce a threshold response is plotted in decibels re  $20 \mu\text{Pa}$  against the frequency of the pure tone stimulus. Results are from adult *Pseudemys*. Temp. =  $22^\circ\text{C}$ . The crosses, joined by the dashed curve are the mean auditory thresholds obtained by behavioural measurements on four *Pseudemys*, and taken from data of Patterson (1966).

Examples of frequency–threshold curves for nerve fibres from one animal are illustrated in Fig. 4. The frequency co-ordinate is logarithmic, and the shapes of the tuning curves, which are representative of the majority obtained, are seen to be roughly symmetrical about the c.f. The crosses, connected by the interrupted line, represent the auditory sensitivity measured by Patterson (1966) for *Pseudemys* using a behavioural technique. Each cross is the mean behavioural threshold for four different animals. The tuning curves for the nerve fibres cover most of the auditory range and the threshold at the c.f. for each of the fibres is comparable to the behavioural curve. The results illustrated in Fig. 4 were from the most sensitive preparation that we observed. The collected sensitivities for nerve fibres from this and other animals are shown in Fig. 5, each type of symbol corresponding to a different animal. There was some scatter of the sensitivities among the preparations, although most fell between 35 and 70 db s.p.l. It is our impression that the higher sensitivities

correspond more closely to the true performance of the intact cochlea, and that the preparations with lower sensitivities may reflect a deterioration in the state of the cochlea during dissection, as the insensitive preparations all came from early experiments. For any one animal, the spread of thresholds at a given frequency spanned a range of only about 10–20 db, which supports the idea that there was no serious deterioration in the condition of a preparation during the course of an experiment.

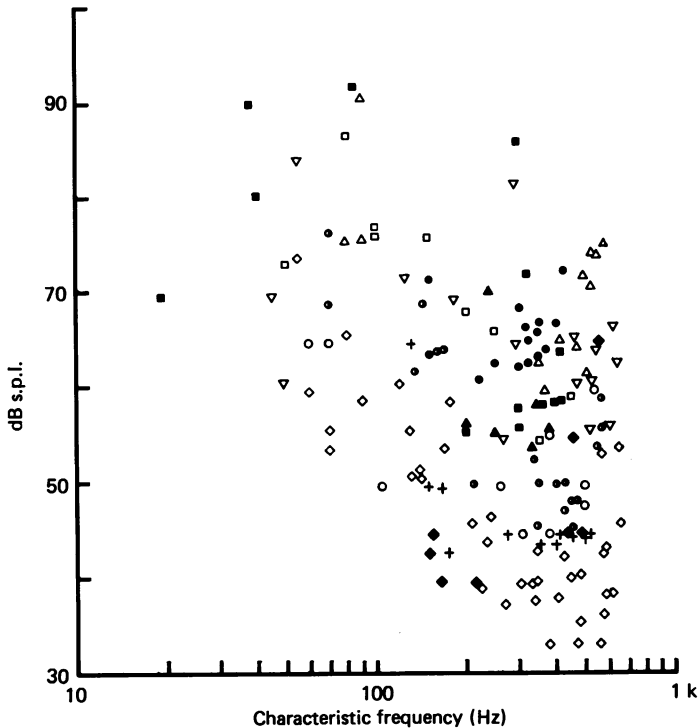


Fig. 5. Collected results of minimum pure tone thresholds for single auditory nerve fibres in the turtle. For each fibre the sound pressure at the tympanum required to generate a threshold response for a stimulus at the fibre's characteristic frequency (c.f.) is plotted against the c.f. Data from eleven experiments, different symbols representing different animals.

Despite the variation in sensitivity from one animal to another, there was no obvious correlation with variations in the sharpness of the frequency–threshold curves.

One way of characterizing a filter curve is in terms of its quality factor or 'Q' value, defined by

$$Q = \frac{f_c}{f_1 - f_2}, \quad (4)$$

where  $f_c$  is the characteristic frequency and  $f_1$  and  $f_2$  are the frequencies above and below  $f_c$  at which the gain of the filter relative to  $f_c$  has fallen by a given amount. It has been a common practice (Kiang *et al.* 1965) in describing frequency–threshold curves of auditory nerve fibres for  $f_1$  and  $f_2$  to be the frequencies at which the threshold sound pressure is 10 db above that at  $f_c$ , so yielding the  $Q_{10\text{db}}$  value. In other applications it may be more useful to measure  $f_1$  and

$f_2$  at the half-power point, which is an amplitude gain of  $1/\sqrt{2}$  or  $-3$  db relative to that at  $f_c$ . For certain kinds of filter, the  $Q_{3\text{db}}$  value then appears in other descriptions of the filter system such as its transient response. In a later section of this paper, the  $Q_{3\text{db}}$  will be used, but for the present purpose, the  $Q_{10\text{db}}$  will be retained to describe the frequency-threshold curves of auditory nerve fibres, in order that these values should be comparable with the data on the mammalian auditory nerve.

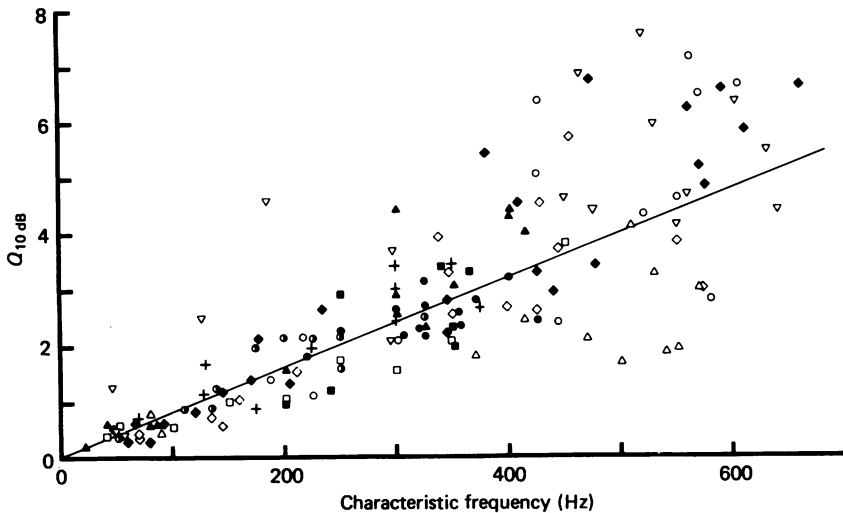


Fig. 6. Collected results for the sharpness of tuning of single auditory nerve fibres in the turtle. The sharpness of tuning for each fibre assessed by the  $Q_{10\text{db}}$  value of its frequency-threshold curve plotted on ordinate against the characteristic frequency (c.f.) of the fibre.  $Q_{10\text{db}}$  given by: c.f./band width of frequency-threshold curve 10 db above minimum threshold. Data from eleven experiments, different symbols for different animals. Note frequency axis is linear. The line was drawn through the points by eye and represents a constant 10 db band width of 125 Hz for the frequency-threshold curves.

The collected  $Q_{10\text{db}}$  values for the nerve fibres are plotted in Fig. 6 against the characteristic frequency for each fibre with different symbols representing different preparations. It should be noted that the frequency axis is linear and hence the mean  $Q_{10\text{db}}$  is seen to increase approximately linearly with  $f_c$ , varying from 0.25 at 30 Hz up to 7 at 600 Hz. The linear variation of mean  $Q_{10\text{db}}$  with the characteristic frequency  $f_c$  can be described by

$$Q_{10\text{db}} = kf_c. \quad (5)$$

The slope,  $k$ , of the line drawn through the points in Fig. 6 is  $8 \times 10^{-3} \text{ Hz}^{-1}$ . This description indicates that the frequency-threshold curves have a constant 10 db band width which is independent of the c.f. of the fibre. The mean band width, given by  $(k)^{-1}$ , is 125 Hz; the scatter of the points increases with c.f., which is equivalent to a constant error in  $k$  of about  $\pm 50\%$ . Thus for a given c.f. the 10 db bandwidth of the frequency-threshold curve can range from about 83 to 250 Hz. Even the broadest of the frequency-threshold curves obtained in the turtle are sharp compared to the mammal in this frequency range, and the average  $Q_{10\text{db}}$  is a factor of two or more larger than those at the same frequency in the mammal (for collected mammalian results see Evans, 1975).

Much of the scatter in the  $Q_{10\text{ dB}}$  values arose within a preparation rather than between preparations and seemed to be unconnected with the sensitivities of the fibres. This was demonstrated on several occasions when consecutive nerve fibres with similar c.f.s but  $Q_{10\text{ dB}}$  values differing by up to a factor of two were encountered on a given track through the auditory nerve. As an example, three consecutive fibres recorded in one experiment had frequency-threshold curves with c.f.s of 425, 455 and 428 Hz, and  $Q_{10\text{ dB}}$  values of 2.6, 5.7 and 4.5 respectively. The sensitivities of the fibres at their c.f. differed by less than a factor 2 and were all between 45 and 50 db s.p.l.

*General description of electrical responses recorded in the basilar papilla*

The basilar papilla is composed of auditory nerve terminals, hair cells and supporting cells. When an intracellular electrode was advanced through the papilla from the scala tympani one of two patterns of response to sound could be recorded from the cells penetrated. These are illustrated in Figs. 7 and 8, and originate, we believe, from nerve terminals and hair cells respectively.

The responses attributed to the terminals of the auditory nerve afferents (Fig. 7) were usually obtained just after the intracellular electrode had entered the papilla, and consisted of a rectified form of the sound wave that could trigger action potentials. The cells typically had resting potentials of  $-60$  to  $-65$  mV, and, in the absence of deliberate sound stimulation, the recordings were characterized by the presence of randomly occurring brief depolarizations. These could often trigger action potentials, as is seen in Fig. 7*A*. With suprathreshold tone bursts (Fig. 7*B*), the responses were synchronized to the cycles of the sound stimulus, and the 'phase-locking' of the action potentials is clearly shown in the spike histogram for the same cell in Fig. 7*C*.

The spontaneous potentials in this cell were 8–10 mV in amplitude, and all had a similar time course, each consisting of a rapid rise followed by a decay of time constant about 1 ms. Similar spontaneous potentials of mean amplitude 4 mV or more were seen in other recordings of this type. Although about an order of magnitude larger and faster, they are reminiscent of the miniature end-plate potentials recorded at the neuromuscular junction (Fatt & Katz, 1952), and it is possible that they too arise from the release of single packets of transmitter from a presynaptic cell. It would seem likely that they are responsible for the spontaneous firing rate in auditory nerve fibres.

A second pattern of electrical response (Fig. 8), which we attribute to the hair cells, was encountered when the electrode had been advanced further into the papilla. These cells gave periodic responses which followed the wave form of the sound stimulus, and were graded with the intensity and frequency of the sound. For a given cell the response was sharply 'tuned' and the largest voltage excursion was obtained for a stimulating frequency characteristic of that cell. Fig. 8 shows averaged responses of a hair cell to tone bursts at various intensities at close to the characteristic frequency (274 Hz). The response during the tone burst was sinusoidal at low intensities and its amplitude was proportional to the sound pressure. With increasing intensity the amplitude increased to a saturating level of 34 mV peak-to-peak. In Fig. 8, the responses apparently continue beyond the time at which the

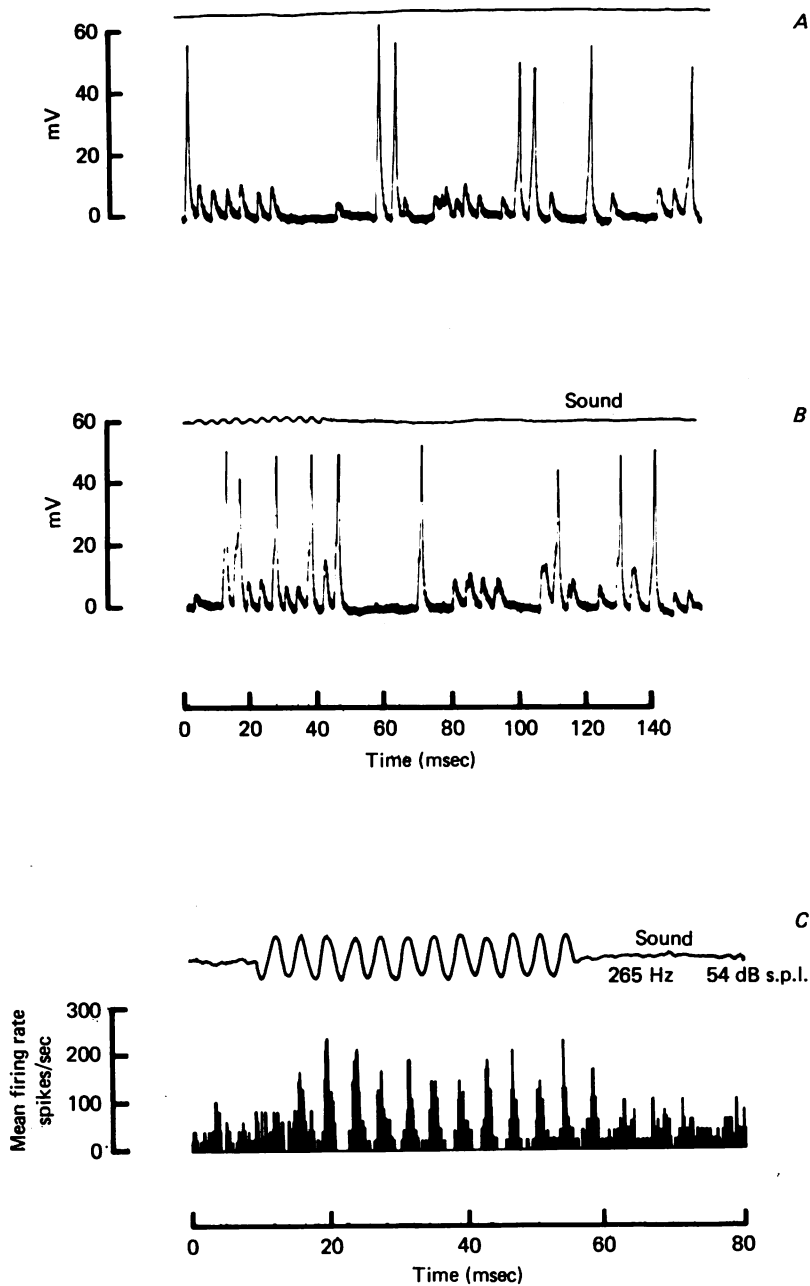


Fig. 7. Intracellularly recorded responses of cell presumed to be terminal of an auditory nerve afferent. Records from cell without deliberate sound stimulation (*A*) and in the presence of a tone at 265 Hz, 54 db re  $20 \mu\text{Pa}$ , (*B*). The upper trace in *A* and *B* is the sound monitor. Voltage expressed relative to the resting potential which was  $-63 \text{ mV}$ . Note the spontaneous potentials which can sometimes trigger impulses. *C*, histogram to show phase-locking of impulses was constructed from 290 responses similar to that in *B*. The sound stimulus in *B* and *C* was the same and at the characteristic frequency of the cell. Temp.  $21^\circ\text{C}$ .

tone burst was switched off, and the potential can be seen to undergo damped oscillations which are most prominent at the lowest intensities. It is thought that these oscillations are a consequence of the tuning of the cell's response, as will be discussed in a later section (see p. 106).

In a number of experiments we injected cells which gave responses similar to those in Fig. 8, with the fluorescent dye Lucifer yellow in order to establish their identity firmly. Although the fraction of stained cells recovered was low (about 30%)

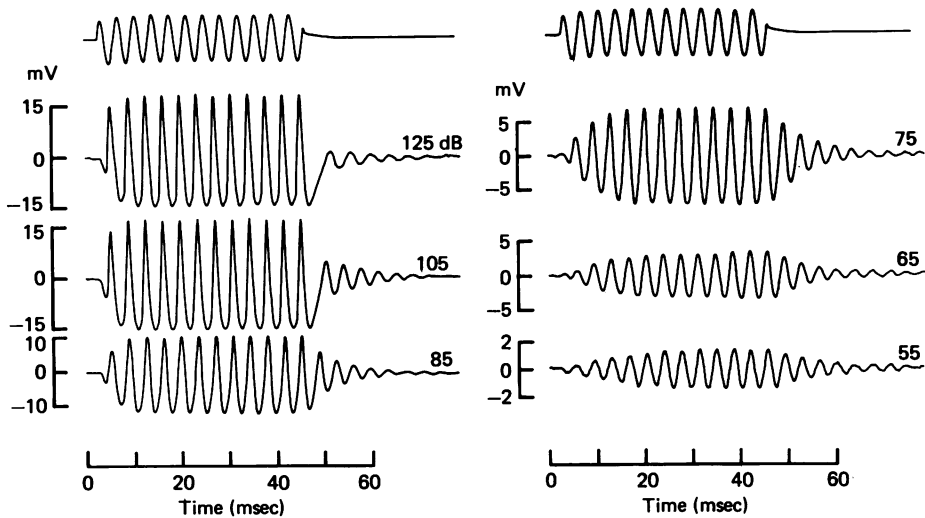


Fig. 8. Intracellularly recorded response of a hair cell to tone bursts at 276 Hz close to its characteristic frequency at various intensities. At each intensity, between 16 and 128 responses have been averaged. Number by each response gives the sound pressure expressed in decibels relative to  $20 \mu\text{Pa}$ . (20 db is equivalent to a tenfold change in sound pressure.) Voltages are with respect to the resting potential, which was  $-54 \text{ mV}$ ; maximum peak-to-peak response of cell,  $34 \text{ mV}$ . The top trace on the left and right is the sound monitor. The tone burst was untapered. Temp.  $21.5^\circ \text{C}$ .

those that were dye-marked were all identifiable as hair cells in transverse sections of the cochlea. In three cases, the dye had diffused into the cilia, which were visible as they were clumped together in a bundle. One example of a marked cell which has the cilia stained, is shown in Pl. 2.

It will be assumed, on the dye-marking evidence, that cells with properties similar to the one illustrated in Fig. 8 are all hair cells. There were several other features of this type of recording which distinguished it. Thus, for example, there was never any evidence of generation of action potentials, or spontaneous potentials of the kind observed in the nerve terminal recordings. However, the hair cell recordings were characterized by a continuous narrow-band noise several millivolts in amplitude. The properties of this noise will be described in detail later in the paper (see p. 112).

All hair cell recordings were associated with large and stable resting potentials, and on loss of a penetration, the response and the noise vanished abruptly along with the resting potential. The 'cochlear microphonic' recorded from just outside the cell (but with the electrode still in the basilar papilla) was 50–100 times smaller

than the intracellularly recorded responses at the same sound pressure. This would argue against the observed potentials being electromechanical artifacts resulting simply from movements of the electrode tip. In the most stable recordings the cells had resting potentials between  $-45$  and  $-55$  mV ( $-50.1 \pm 1.3$  mV, mean  $\pm$  s.e. of mean,  $n = 7$ ) and gave maximum responses at the characteristic frequency of 30–45 mV peak-to-peak. Some of the features of the recordings from the seven cells with the largest responses are presented in Table 1.

TABLE 1. Electrical properties of hair cells with large responses

$R_{\max}$ (mV)	$E_r$ (mV)	c.f. (Hz)	Sound pressure for 1 mV response at		$Q_{10\text{ db}}$	Temp. ( $^{\circ}\text{C}$ )
			c.f. (db s.p.l.)	10 db bandwidth (Hz)		
34	-50	94	73.7	94	1.00	22.0
45	-55	100	51.5	248	0.40	21.0
40	-48	250	59.4	196	1.27	19.5
34	-54	274	46.3	114	2.46	21.5
36	-50	311	48.4	130	2.39	21.0
36	-48	346	52.5	326	1.01	21.0
28	-46	425	60.7	240	1.77	25.0

c.f., characteristic frequency;  $R_{\max}$ , saturated peak-to-peak response at c.f.;  $E_r$ , resting potential. Figures in columns 3–6 derived from measurements on 1 mV iso-response tuning curves;  $Q_{10\text{ db}}$  = characteristic frequency/10 db band width.

The properties of a cell often appeared to be linked to the stability of the recording, or its quality as reflected by the maximum size of response obtainable from the cell. The cell was judged to be acceptable for most purposes if it was capable of giving at least 15 mV peak-to-peak. This threshold is somewhat arbitrary (it represents a third of the largest response seen), but it correlated remarkably well with a consistent resting potential. In recordings from twenty-three cells which fell into this category, the resting potential was  $-48.9 \pm 4.7$  mV (mean  $\pm$  s.d.). Some of the scatter in the resting potentials and size of the responses can be seen in the results given in Table 3.

During the course of a penetration through the basilar papilla, the intracellular electrode often impaled cells with larger resting potentials ( $-70$  to  $-80$  mV) and negligible response to sound. In addition to these recordings, which were presumably from supporting cells, a large stable potential of about  $-80$  mV was often observed at the end of a penetration if the electrode was pushed right through the hair cell layer. It is conceivable that at this stage, the electrode was embedded in the tectorial membrane; further advancement of the electrode, resulting in a loss of the potential, always brought it into the cochlear duct. The endocochlear potential was never more than a few millivolts with respect to the perilymph, and this is in agreement with the results of Schmidt & Fernandez (1962) who measured endocochlear potentials of  $-2$  to  $+5$  mV in intact turtles.



*Intensity–amplitude relations for hair cells*

The relationship between sound pressure and the amplitude of a hair cell's response is presented in Fig. 9 for six different cells. In each experiment the ear was stimulated with tone bursts at close to the characteristic frequency for the cell. The peak-to-peak amplitude,  $V$ , of the averaged response at a given intensity has been normalized to the saturated amplitude  $V_{\max}$ , obtained with a very intense sound;

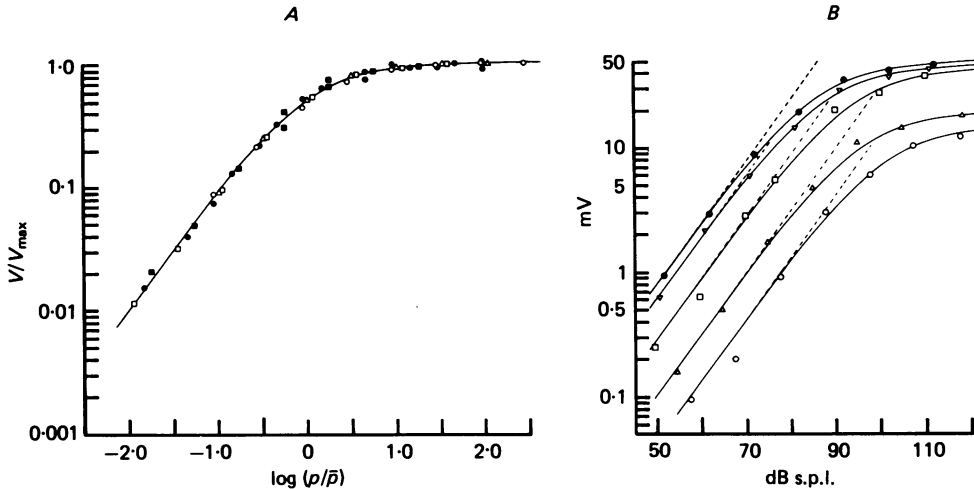


Fig. 9. *A*, intensity–amplitude relations for six hair cells. For each cell, the peak-to-peak amplitude of the response as a function of sound pressure was measured for tone bursts at a frequency near the characteristic frequency of the cell. The response as a fraction of the maximum response is plotted on the ordinate, and the sound pressure normalized to  $\bar{p}$  (that required to produce a half-maximal response) is plotted on the abscissa. The smooth curve is an empirical fit based upon eqn. (6) in the text. The values of  $\bar{p}$  and the stimulating frequencies are given in Table 2. *B*, intensity–amplitude relations at different frequencies for one hair cell. The peak-to-peak response is plotted against the sound pressure in db re  $20 \mu\text{Pa}$ . Frequencies: ●, 100 Hz (the characteristic frequency of the cell); ▽, 58 Hz; □, 33.5 Hz; △, 500 Hz; ○, 840 Hz. The continuous curves through the points were empirical fits based upon eqn. (6) in the text. The dashed lines describe the linear relationship between sound pressure and response, and asymptote to the continuous curves at low sound pressure. (20 db is equivalent to a tenfold change in sound pressure.) Resting potential  $-55 \text{ mV}$ . Temp.  $21^\circ \text{C}$ .

since different cells had different sensitivities, the sound pressure,  $p$ , in each experiment has also been scaled to that required to produce a half-maximal response ( $\bar{p}$ ). These normalizations allow the points from different experiments to be superimposed, and it can then be seen that the form of the saturation is similar for all cells. The smooth curve, which is an empirical fit to the points, is a rectangular hyperbola described by the equation

$$\frac{V}{V_{\max}} = \frac{p}{p + \bar{p}} \quad (6)$$

Values for the half-saturation sound pressure,  $\bar{p}$ , for these experiments are given in Table 2. The mean value of  $\bar{p}$  was 86 db s.p.l.

For low sound pressures the response of a cell was found to be directly proportional

to sound pressure, as may be inferred from the limiting slope of the intensity amplitude plots in Fig. 9A. The generalization of linearity held for most hair cells if the sound produced a response of less than about 2 mV peak-to-peak. From the small responses it is thus possible to calculate a linear sensitivity,  $S$ , for a cell, given by the root mean square voltage response divided by the sound pressure (which is also an r.m.s. value) for a tone at the characteristic frequency. The most sensitive cells had values of  $S$  in the range 30–90 mV/Pa (Table 2).

TABLE 2. Sound sensitivities of hair cells

Symbol	$f$ (Hz)	$\bar{p}$ (db s.p.l.)	$S$ (mV/Pa)
△	120	83.2	56.6
●	250	86.7	32.5
◐	250	84.9	36.1
○	275	75.7	88.8
■	350	96.3	5.3
□	450	88.2	18.4

Values obtained from averaged responses to tone bursts at frequency  $f$  (close to the c.f.) at various intensities. Results plotted in Fig. 9, each symbol representing a different cell;  $\bar{p}$ , sound pressure for half-saturated response, in decibels re 20  $\mu$ Pa;  $S$ , linear sensitivity calculated as described in text.

If the amplitude of a cell's response as a function of sound pressure was examined away from the c.f. the response exhibited a similar form of saturation, although the saturated response  $V_{\max}$ , was smaller than at the c.f., and a higher sound pressure was required to reach it, i.e. the value of  $\bar{p}$  was larger than at the c.f. This can be seen in Fig. 9B which gives sound pressure–amplitude relations for a single cell at five different frequencies. The upper set of points (filled circles) represent the responses at the c.f. of the cell (100 Hz); the open symbols are for frequencies on either side of the c.f. The smooth curve calculated from eqn. (6) fits the points for frequencies other than the c.f. with reduced values of  $V_{\max}$  and increased  $\bar{p}$ . A possible explanation for this type of behaviour has been put forward previously in terms of a dual mechanism for achieving frequency selectivity (Fettiplace & Crawford, 1978). It was envisaged that the saturation process was sandwiched between the two filters whose form could be inferred from the variations in  $\bar{p}$  and  $V_{\max}$  respectively as a function of frequency. This is only completely correct if the fundamental in the cell's response is plotted and if both filters are linear and the saturation is instantaneous. In reality the second filter is markedly non-linear (Fettiplace & Crawford, 1978; Crawford & Fettiplace, 1980,) which may contribute to the variation in  $V_{\max}$  and  $\bar{p}$ , particularly near the c.f.

The interrupted lines in Fig. 9B represent the linear relationship between the amplitude of the response and the sound pressure, and asymptote to the continuous curves at low sound pressure. It should be noted that if the response at a given sound pressure is in the linear range at the c.f., it will also be linear at other frequencies.

*Non-linearities in the wave form of the hair cell's response*

For low and moderate sound intensities the voltage signals generated in a hair cell were approximately sinusoidal for all frequencies of stimulation. This can be seen in the segments from the low intensity frequency sweeps in Fig. 12. At high intensities, however, the shape of the response wave form displayed a number of

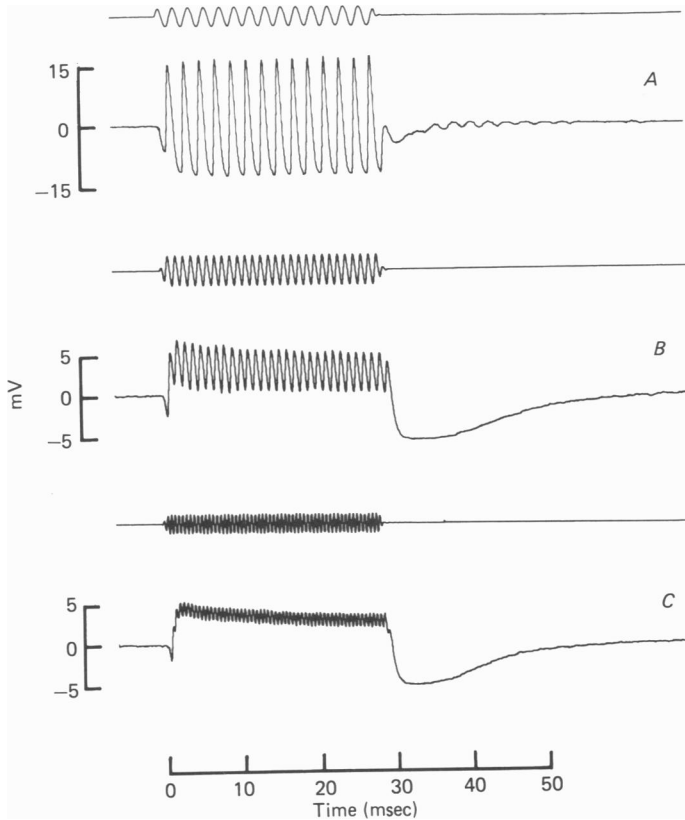


Fig. 10. Periodic and sustained components of a hair cell's response to tones at high intensity as a function of the frequency of stimulation. Frequencies and sound pressures: (A), 500 Hz, 120 db; B, 1 kHz, 122.5 db; C, 2 kHz, 125 db; sound pressure expressed relative to  $20 \mu\text{Pa}$ . The upper trace of each pair is the sound monitor. Thirty-two responses have been averaged at each frequency. Cell has characteristic frequency 425 Hz; voltages given with respect to the resting potential which was  $-46 \text{ mV}$ . Temp.  $25^\circ\text{C}$ .

non-linear features, the type of non-linearity in a given cell depending upon the frequency of stimulation relative to the characteristic frequency.

At the characteristic frequency, despite an amplitude saturation, the signals remained surprisingly sinusoidal, and only at the highest sound pressures was a departure from this observed; then the depolarizations became narrower in that the cell remained depolarized for a shorter time than half the period, while the fraction of the period spent on the hyperpolarizations was increased. This type of distortion is visible at the two highest sound pressures in Fig. 8; it is thought to be related to

the distortion which occurs at frequencies well below the c.f. (Fettiplace & Crawford, 1978).

A second type of non-linearity consisted of a maintained depolarizing component which became more pronounced relative to the periodic signal at high frequencies. The phenomenon is illustrated in Fig. 10 which shows averaged responses to tone bursts at three frequencies above the c.f. of the cell. The upper record (Fig. 10*A*) is

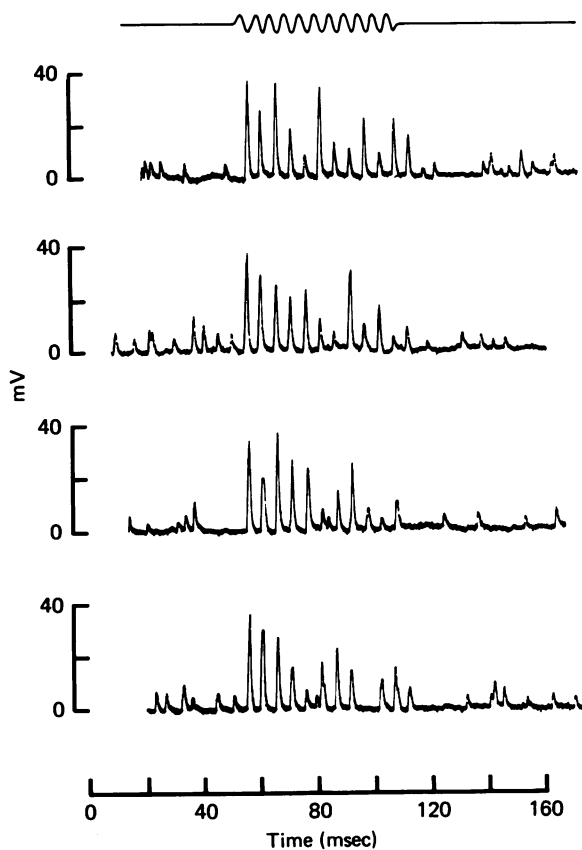


Fig. 11. Intracellularly recorded response from a cell presumed to be an auditory nerve terminal. The responses are shown to four consecutive tone bursts at 200 Hz, 94 db re 20  $\mu$ Pa. The spiking mechanism failed earlier in the recording; note the fluctuation in the size of the response to a given cycle of the sound. Voltage scale is relative to the resting potential, which was  $-62$  mV. Top trace is sound monitor.

a response at 500 Hz, close to the c.f.; the depolarizing phase, measured from the resting potential, was 15.8 mV and the hyperpolarizing phase was 12.8 mV. The mid point of the responses, half-way between the peaks and dips, was thus 1.5 mV positive to the resting potential. The middle record (Fig. 10*B*) is the response of the cell at 1 kHz. At this frequency the shift, measured in the same way, was initially 4.1 mV but declined during the tone burst to 2.6 mV. For the response at 2 kHz (Fig. 10*C*), the depolarizing shift was initially 4.5 mV, declining by the end of the tone to 3 mV.

The steady component of the response may reflect a rectification in the periodic signal which, at the higher frequencies, is then presumably smoothed or low-pass filtered, thus attenuating the periodic component relative to the steady component (Russell & Sellick, 1978). This could account for the form of the responses in Fig. 10B

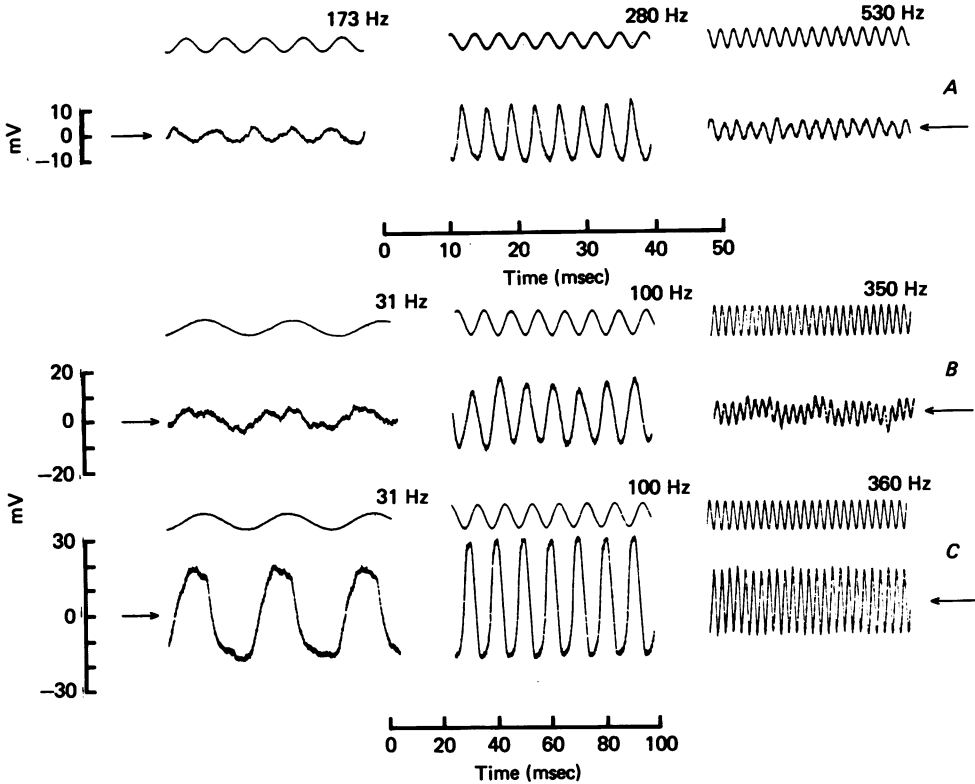


Fig. 12. Segments from frequency sweeps at constant intensity to illustrate the frequency selectivity for two hair cells. For each sweep a section close to the c.f. of the cell, and sections above and below the c.f. are shown. *A*, sound pressure for all three frequencies is 81 db re 20  $\mu$ Pa; c.f. of cell, 274 Hz; resting potential -54 mV. *B*, sound pressure at c.f. is 82 db re 20  $\mu$ Pa; c.f. of cell, 100 Hz; resting potential -55 mV. *C*, same cell as in *B*; sound pressure at c.f. is 112 db re 20  $\mu$ Pa. In each pair of traces, upper one is sound monitor, lower one hair cell voltage. Number above sound monitor gives stimulation frequency. Note in *B* and *C*, sound pressure increases slightly from lowest to highest frequency, due to frequency response of earphone. The voltages are given relative to the resting potential, the arrows indicating the position of the d.c. level before and after the sweep. For both experiments the sound frequency was swept exponentially at a rate of about 1 decade per 20 s.

and *C*. At the c.f., owing to the wave-form distortion which was mentioned previously, a subsequent smoothing of the response would lead not to a depolarizing but rather to a hyperpolarizing steady potential. This would arise because, at high sound pressures, the time that the hair cell spends depolarized is smaller than the time spent hyperpolarized. As an example a time integration of the 500 Hz response in Fig. 10A yields a steady negative potential of 1.8 mV.

The steady component of the responses at 1 kHz and 2 kHz displayed a slight

adaptation or sag, the majority of which occurred with a time constant of about 10 ms. Accompanying the sag during the tone was a hyperpolarization when the tone was terminated. This after-hyperpolarization could be as large as 10 mV.

There was found to be no significant adaptation of the periodic component of the response over a duration of a minute or more, and this enabled us to use continuous tones to examine the tuning of the hair cell, as described in the next section. Nor was the sag in the steady potential, as shown in Fig. 10, observed at stimulating frequencies less than about 1 kHz. It is a phenomenon restricted to high frequencies and in this respect it differs from the adaptation which is sometimes seen in auditory nerve firing.

The nerve fibre adaptation could occasionally be observed in the intracellularly recorded responses from what are presumed to be the nerve terminals. Often, during the course of such a recording, the spiking mechanism would fail, so revealing the form of the underlying synaptic potentials. An example is shown in Fig. 11. Although these potentials fluctuate from one sound presentation to the next, their average size declines during the tone burst. A comparable adaptation has previously been reported by Furukawa & Matsuura (1978) for the excitatory synaptic potentials in the auditory nerve fibres of the goldfish. The probabilistic nature of the synaptic potentials (Fig. 11) is also quite different from the hair cell potentials whose constancy is evident in the responses at the c.f. in Fig. 12.

What has been said so far about the wave forms of the hair cell responses generally applied only to cells with maximum peak-to-peak responses of 15 mV or more. Quite satisfactory, and often stable recordings, could be secured from cells with smaller responses, but the features of the wave form were altered, the most marked difference being that, at the c.f., the responses were more rectified. In addition, the peaking in the wave form at the c.f. was absent and the responses became flat-topped at high sound pressures.

#### *The frequency selectivity of the hair cell's response*

*Iso-response tuning curves.* In all hair cell recordings the size of the periodic signal depended upon the frequency of the sound stimulus, each cell being 'tuned', i.e. responding best at a frequency characteristic of the cell, and giving smaller responses at higher or lower frequencies. Most of our information on the tuning of the response is derived from presentations of a steady tone whose frequency could be continuously varied. Fig. 12 shows examples from three such frequency sweeps at constant sound pressure for two cells with different c.f.s; segments above, below and at the c.f. have been taken from each sweep in order to illustrate the selectivity. In Fig. 12*A* the cell is shown responding near its c.f. (280 Hz) and also on either side of the c.f. at 173 Hz and 530 Hz. In each pair of traces the upper one gives a monitor of the sound pressure, and the lower one the recording from the intracellular electrode. Fig. 12*B* and *C* show sections from two frequency sweeps at different intensities for another cell, illustrating the responses near the c.f. (100 Hz) and also at 31 Hz and 350 Hz. From the traces in Fig. 12*C* it can be seen that at the higher sound intensity the cell was not as selective as at the lower intensity (see also Fig. 13*B*). This result is similar to the broadening of the iso-intensity curves found by Rose, Hind, Anderson & Brugge (1971) for mammalian auditory nerve fibres.

In order to compare the frequency selectivity of the hair cell's response with that for the auditory nerve fibres, it is necessary to express the two in an analogous fashion. The tuning curves that have been measured for a given nerve fibre represent the sound pressure required to elicit a constant increment in the firing rate. Frequency selectivity curves at a constant level of response were generated for the hair cells as follows: at a number of different frequencies intensity–amplitude relations were con-

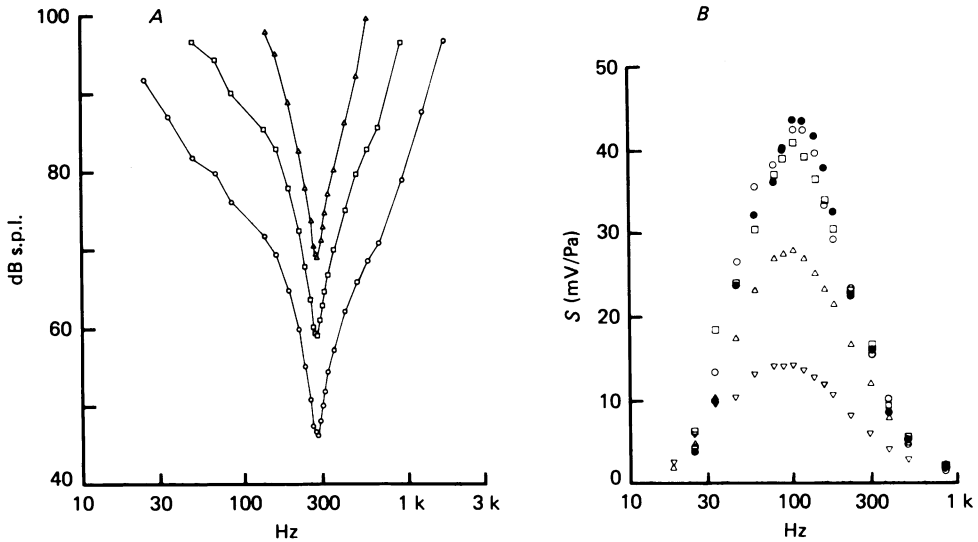


Fig. 13. *A*, iso-amplitude contours for hair cell of Fig. 12 *A*. The ordinate is the sound pressure (expressed in decibels re  $20 \mu\text{Pa}$ ) required to produce a constant amplitude of response in the hair cell as a function of the stimulation frequency on the abscissa. The three curves are for three different amplitude criteria, whose peak-to-peak values were:  $\circ$ , 1 mV;  $\square$ , 4 mV;  $\triangle$ , 10 mV. Data points were interpolated from intensity–amplitude plots at the various frequencies. For details of recording see legends for Fig. 8 and Fig. 12 *A*. *B*, iso-intensity frequency response curves for a hair cell. The sensitivity of the cell (r.m.s. voltage divided by the sound pressure) is plotted against the stimulation frequency; the results were obtained from frequency sweeps at constant intensity. Sound pressures in decibels re  $20 \mu\text{Pa}$ :  $\bullet$ , 52 db;  $\circ$ , 62 db;  $\square$ , 72 db;  $\triangle$ , 82 db;  $\nabla$ , 92 db. Intensity–amplitude curves at some frequencies are given for this cell in Fig. 9 *B*. Note that for the two lowest intensities, the points are virtually superimposable; at these intensities the responses were linear with sound pressure at all frequencies. Same cell as Fig. 12 *B* and *C*; see legend to Fig. 12 for details of recording.

structed (for examples of these see Fig. 9 *B*), and the sound pressure required to produce a given peak-to-peak response, say 1 mV, in the hair cell at these various frequencies was then interpolated from the plots. Fig. 13 *A* shows iso-response curves obtained in this way for the hair cell of Fig. 12 *A*: the three curves correspond to criterion responses of 1, 4 and 10 mV peak-to-peak respectively. For all the curves the sound pressure needed to elicit the required response was a minimum at 274 Hz, and rose on either side of this optimum frequency. In several other cells, the optimum frequency did not vary, within experimental error, between the 1 and 10 mV iso-response curves.

The sharpness of tuning of the iso-response curves was evaluated in the same way as was done for the frequency threshold curves for the auditory nerve fibres. For the 1, 4 and 10 mV iso-response curves in Fig. 13*A* the 10 db bandwidth was 114, 114 and 109 Hz respectively. Each band width was then divided into the c.f. to give the  $Q_{10\text{ db}}$  value, which is 2.46 for the 1 and 4 mV curves, and 2.57 for the 10 mV curve. It is likely that this slight increase in the  $Q$  value for the larger response criterion is significant, as it was consistently observed in the other cells examined, but it is small compared to the variation in  $Q$  between different cells. Thus it is unnecessary to know the exact size of the response in a hair cell at 'threshold' for the nerve fibres in order to compare their tuning curves. For the other cells details of iso-response curves for a single criterion response of 1 mV will be given. These iso-response curves for seven cells are collected in Fig. 14, and the constants for the curves are given in Table 1. Several conclusions can be drawn from these results: (a) each hair cell had a single c.f., which was different for different cells; (b) the sound pressure required to generate a response of 1 mV at the c.f. varied from 46.3 db s.p.l. to 73.7 db s.p.l.; these sound pressures fall within the range of 'thresholds' for most of the nerve fibres (see Fig. 5), and this suggests that the hair cells might be producing of the order of 1 mV at the nerve fibre 'threshold'; (c) there was some variation in the sharpness of tuning between hair cells. A similar divergence in tuning was observed in the frequency threshold curves of the nerve fibres, but most of the 10 db band widths fell within the range 83–250 Hz. The band widths of the iso-response curve of all the hair cells in Table 1, except for cell number 6 ( $f_c = 346$  Hz) were within this range. For the hair cells, the mean and standard deviation of the inverse bandwidth,  $k$ , (eqn. (5)) was  $6.21 \pm 2.84 \times 10^{-3}$  Hz $^{-1}$ , as compared to  $8 \times 10^{-3}$  Hz $^{-1}$  for the nerve fibres. This mean is equivalent to a 10 db band width of 161 Hz. From these results we would conclude that the frequency selectivity of the hair cells is comparable to that of the nerve fibres. Russell & Sellick (1978) have reached the same conclusion about the inner cells in the guinea-pig cochlea, which, they report, are as sharply tuned as the auditory nerve fibres in that animal.

For comparing the sharpness of tuning of the hair cells and auditory nerve fibres, only the best recordings have been taken into consideration. This was done because we felt that the observed tuning was related to the quality of the recording, and furthermore could change during the course of an experiment. Some of the difficulties in determining the tuning properties of a hair cell are illustrated by considering the case of the more broadly tuned cell 6 in Table 1. A few minutes after beginning to record from the cell, an iso-intensity frequency sweep at 74 db s.p.l. generated a maximum response of 1.7 mV at the c.f., which was 226 Hz. The resting potential of the cell at this point was  $-34$  mV, and the  $Q_{3\text{ db}}$  of the tuning curve was 0.67. About 5 min later, the resting potential had increased to  $-48$  mV, and a frequency sweep at the same intensity gave 10.6 mV at the c.f., which had increased to 328 Hz. The  $Q_{3\text{ db}}$  of the tuning curve was now 2.73. A third frequency sweep several minutes later at the same intensity now gave 13.3 mV at the c.f., 346 Hz, and the  $Q_{3\text{ db}}$  was 3.22. This final improvement had been accomplished without any further change in the resting potential. The properties of the iso-response curve for the cell, given in Table 1, were derived at about this point in the recording, and it is possible that the real sharpness of tuning and c.f. of the cell were still underestimated. Thus the  $Q$  value derived from the terminal oscillations to tone bursts, as described in the next section, was even higher later in the experiment.

*Iso-intensity tuning curves.* For most of the hair cells, less complete measurements were available and it was not possible to construct sets of iso-response curves. For almost all the cells, however, a linear iso-intensity curve could be obtained from the



response to a low intensity frequency sweep which generated a response of less than about 2 mV at the c.f. of the cell. The linearity was sometimes verified by a second sweep at an intensity 10 db higher or lower. A low sound pressure which produces responses in the linear range at the c.f. will also generate linear responses at other frequencies (Fig. 9B). Hence the form of the iso-intensity frequency response curve

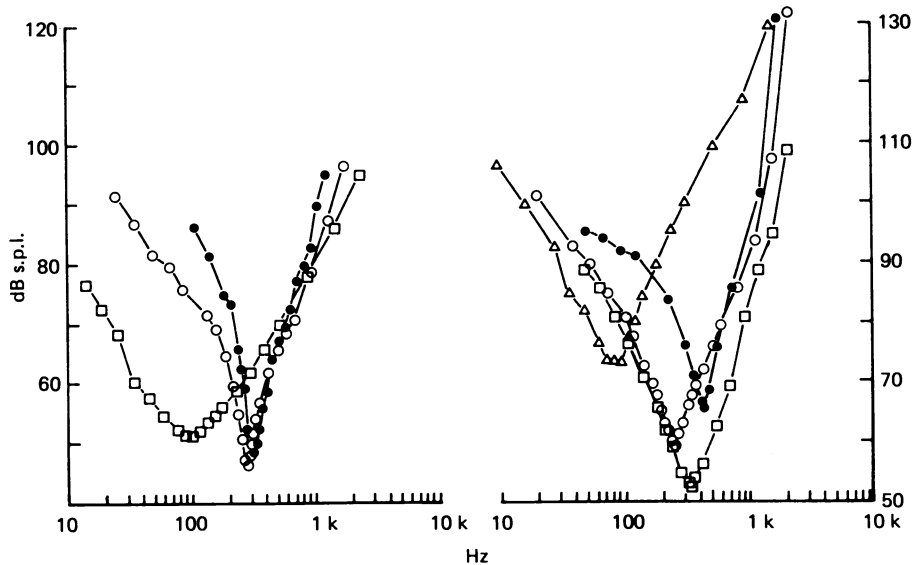


Fig. 14. Collected iso-amplitude tuning curves for seven hair cells. The ordinate is the sound pressure (expressed in db re  $20 \mu\text{Pa}$ ) required to produce a constant amplitude of 1 mV peak-to-peak as a function of the stimulation frequency on the abscissa. Note that there is a 10 db difference between the left and right sound pressure axes. The characteristics of the tuning curves, along with some other properties of the seven cells, are presented in Table 1.

will be independent of the sound pressure at low intensities. This is demonstrated for one cell in Fig. 13B, which gives iso-intensity curves at five sound pressures increasing in 10 db steps. For each set of points, the response has been scaled by the sound pressure and so the ordinate expresses the sensitivity of the cell as a function of frequency. The two lowest sound pressures, denoted by the closed and open circles, produced responses of 0.95 and 2.95 mV peak-to-peak respectively at the c.f. The two sets of points are superimposable to within the error of the measurements and fall along a common curve which we have termed the linear iso-intensity curve. At higher sound pressures there is a progressive reduction in sensitivity, most prominent in the region of the c.f., which blunts the tip of the curve. The shape of the linear iso-intensity curve near the tip is identical to the 1 mV iso-response curve for the same cell, although there are differences between the two curves on the skirts.

When all the cells were taken into consideration, including those with smaller responses, the sharpness of tuning of the cells fell broadly into two categories. These are shown in Table 3 which contains details of the tuning properties of twenty-three hair cells. For each cell the degree of tuning of the linear iso-intensity curve has been evaluated both in terms of the  $Q_{10\text{db}}$  and  $Q_{3\text{db}}$  values calculated using eqn. (4).

The two categories of tuning are illustrated by considering for example the nine cells with c.f.s between 215 and 311 Hz. Four of these cells were sharply tuned like the nerve fibres, and had a  $Q_{3\text{ dB}}$  of 4.03–8.40; five others were more broadly tuned, with a  $Q_{3\text{ dB}}$  of about 1–1.5. A similar division may be seen in the remainder of the cells, although the categories are less well defined because of the fact that

TABLE 3. Tuning characteristics of hair cells obtained from linear iso-intensity curves

$R_{\text{max}}$ (mV)	$E_r$ (mV)	c.f. (Hz)	$Q_{10\text{ dB}}$	$Q_{3\text{ dB}}$
34	-50	94	1.00	2.35
45	-55	100	0.40	1.16
32	-50	111	—	1.66
26	-43	110	0.39	1.00
18	-50	129	—	0.66
16	-39	130	0.35	1.06
20	-50	158	0.46	1.59
22	-51	177	0.48	0.99
—	-52	196	0.52	1.41
20	-43	215	0.52	0.94
18	-59	229	0.30	1.43
24	-47	239	0.33	1.42
40	-48	250	1.27	4.03
14	-50	266	0.61	1.40
18	-48	274	2.36	7.21
36	-54	274	3.47	8.40
20	-44	304	0.58	1.54
36	-50	311	2.39	5.87
36	-48	346	1.01	3.22
20	-42	400	0.86	1.74
28	-46	425	1.77	5.31
19	-57	431	2.79	6.13
—	-50	485	0.85	3.33

c.f., characteristic frequency;  $R_{\text{max}}$ , saturated peak-to-peak response at c.f.;  $E_r$ , resting potential;  $Q_{10\text{ dB}}$  and  $Q_{3\text{ dB}}$  calculated using eqn. (4).

there are fewer sharply tuned cells in any other frequency range. In most cases, cells with smaller responses had broader tuning curves, although there were some exceptions to this generalization. On the evidence that the quality factor of a hair cell can increase during an experiment, moving from the broad category into the sharp category, it is tempting to suppose that the broad tuning curves did not reflect the true tuning ability of those hair cells, but rather were the result of some interference by the electrode.

#### *Tonotopic organization*

The c.f.s of the linear iso-intensity curves for different hair cells varied between 70 and 670 Hz, which covers most of the range of the nerve fibres. The possibility of there being a mapping of frequency into distance on the basilar membrane was examined by measuring the position along the membrane of the tip of the electrode at the end of a recording. A tonotopic organization is indicated by the collected

results of these measurements, which are shown in Fig. 15. The open circles are from measurements on hair cells, with the c.f. of the cell being plotted logarithmically against its distance along the basilar membrane from the apical or lagenar end. The filled circles are measurements on auditory nerve fibres; these were obtained in three experiments in which extracellular recordings were made from nerve fibres in

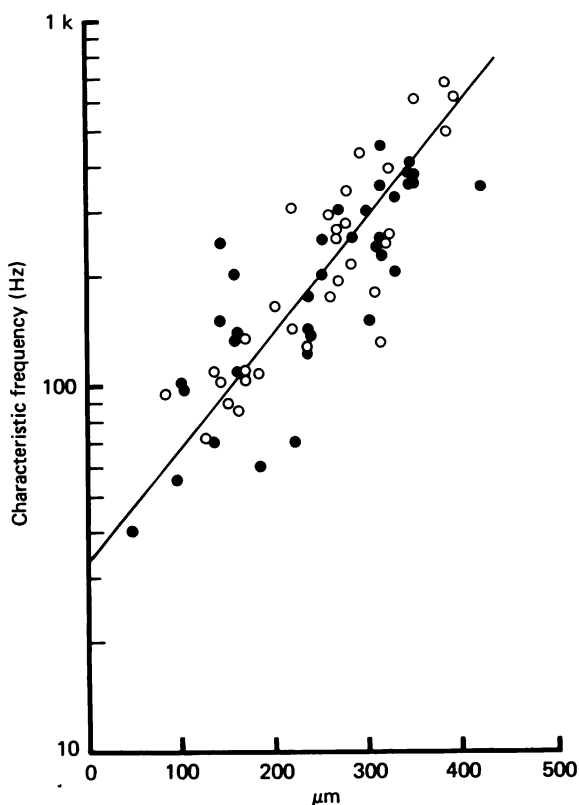


Fig. 15. Tonotopic organisation of hair cells (open circles) and auditory nerve fibres (filled circles) along the basilar membrane. The characteristic frequency of a cell is plotted as a function of the distance of the cell from the apical (lagenar) end of the cochlea. The position of the cell was determined by measuring the position of the electrode at the end of a recording. The total length of the cochlea was also measured. The hair cell measurements from different experiments have been scaled to a constant basilar membrane length ( $700 \mu\text{m}$ ). The nerve fibre measurements were made in three experiments with the extracellular electrode placed in the neural limb (see Pl. 1). Straight line is least squares fit to points.

the neural limb. At this point in the auditory pathway, the fibres have just left the papilla, and are running perpendicularly to the long axis of the basilar membrane (Pl. 1), and so it is likely that the tonotopic mapping is still preserved.

Despite scatter in the results, there is a clear change of c.f. with position, with the low frequencies being located at the apical end and the higher frequencies at the basal end near the saccule. This is the same orientation of the map as occurs in the mammalian cochlea (von Békésy, 1960). The line drawn through the points gives the

relationship between the characteristic frequency,  $f_c$ , of a cell and its distance  $x$ , in  $\mu\text{m}$  along the membrane from the apex, described by:

$$f_c = f_0 e^{x/\lambda}, \quad (7)$$

$f_0$  and  $\lambda$  are constants, with values of 34 Hz and 135  $\mu\text{m}$  respectively; the value of the space constant  $\lambda$  is equivalent to a doubling of the frequency in 94  $\mu\text{m}$ .

With the scatter in the points it is doubtful whether, over the limited frequency range available, it is really possible to distinguish between a linear and a logarithmic map. It would be useful to examine the continuation of the map in the basal 150  $\mu\text{m}$ . So far we have been unable to record from this region of the papilla, as it is normally covered by a branch of the auditory nerve which innervates the ampulla of the posterior semicircular canal. There are two main sources of error in the present measurements which may partly account for the scatter in the points. One is the difficulty of accurately measuring the position of the tip of the electrode in the papilla; some of this arises because the cochlea was normally tilted during an experiment. A more serious source of error would be that, for cells with small responses, the measured c.f. may have been incorrect for reasons described in the previous section.

#### *Hair cell tuning as a resonance phenomenon*

*Responses to tone bursts.* The temporal properties and frequency selectivity of a linear filter are intimately related such that the sharper the tuning of the filter, the more prolonged is its time response. The phenomenon is illustrated by the records in Fig. 8 for a hair cell which was very sharply tuned. The responses to tone bursts at the characteristic frequency were spread out, so that for small responses, the amplitude of the sinusoidal voltage took several cycles to build up to a maximum value during the tone, and the oscillations then continued after the tone burst was ended, with the response amplitude decaying exponentially. The frequency of the terminal oscillations was close to the characteristic frequency of the cell and was unrelated to the frequency of stimulation.

The following analysis is an attempt to relate quantitatively the temporal properties and frequency selectivity of a hair cell, and provides an independent way of assessing the quality factor of the tuning of a hair cell from its responses to tone bursts. For the analysis it is necessary to assume that the system is behaving linearly, and this is probably the case if the cell is producing a response of no more than a few millivolts in amplitude. The analysis is based upon the idea that the temporal response of a hair cell to a tone burst near its c.f. is determined by the shape of its tuning curve near the tip, and that this can be approximated by the spectrum for a second-order resonance filter. The differential equation for the behaviour of such a filter is:

$$\ddot{y} + \gamma\dot{y} + \omega_0^2 y = F(t). \quad (8)$$

This equation could describe, for example, an electrical filter incorporating an inductance, resistance and capacitance, or a mechanical filter comprising a mass, resistance and compliance;  $y$  is the output of the filter, the dot indicating differentiation with respect to time, and  $\omega_0$  and  $\gamma$  are the resonant angular frequency and damping constant of the filter respectively.  $F(t)$  is a driving function, in the present case

representing a tone burst of duration  $T$  and angular frequency  $\omega$ .

$$F(t) = \left. \begin{aligned} F \cos \omega t & \quad 0 \leq t \leq T \\ = 0 & \quad t < 0, t > T. \end{aligned} \right\} \quad (9)$$

The terminal oscillations which occur when the tone burst is switched off are the result of the system being set into free vibration, and their form may be obtained by solving eqn. (8) with  $F(t) = 0$ . For light damping ( $\gamma < 2\omega_0$ ), which is always the case for the hair cell, the solution is an exponentially decaying oscillation:

$$y = A \exp \left[ -\frac{1}{2}\gamma(t-T) \right] \cos [\omega_t(t-T) + \phi] \quad (10)$$

for  $t > T$ .  $A$  and  $\phi$  are constants set by the amplitude and phase of the steady response when the tone is switched off;  $\omega_t$  is the frequency of free vibration, given by

$$\omega_t = \omega_0 \left[ 1 - \frac{1}{(2Q')^2} \right]^{\frac{1}{2}} \quad (11)$$

and is approximately equal to the resonant frequency  $\omega_0$ , for large  $Q'$ .  $Q'$ , the quality factor is defined by

$$Q' = \frac{\omega_0}{\gamma}. \quad (12)$$

The value of  $Q'$  obtained from this analysis is approximately equal to the  $Q$  derived from measurements of the tuning curve;  $Q$  is defined by eqn. (4):

$$Q = \frac{\omega_0}{\omega_1 - \omega_2},$$

where  $\omega_1$  and  $\omega_2$  are the frequencies at which the amplitude has fallen to  $\sqrt{\frac{1}{2}}$  of its maximum value. The discrepancy between the two values of  $Q$  decreases as  $Q$  becomes large, depending upon the system. (For a second order resonance, they differ by 2% for a  $Q$  of 5.) It should be noted that neither definition of the quality factor is strictly correct for a more complicated filter, where it is normally defined in terms of the energy lost within the oscillating system.

The solution to eqn. (8) for the tone burst being switched on is:

$$\begin{aligned} y &= F\mu^{-2} \{ (\omega_0^2 - \omega^2) \cos \omega t + \omega\gamma \sin \omega t \} \\ &\quad - F\mu^{-2} e^{-\frac{1}{2}\gamma t} \left\{ (\omega_0^2 - \omega^2) \cos \omega_t t + \gamma \frac{(\omega^2 + \omega_0^2)}{2\omega_t} \sin \omega_t t \right\} \end{aligned} \quad (13)$$

$$\mu^2 = (\omega^2 - \omega_0^2)^2 + \omega^2 \gamma^2$$

for the initial conditions

$$y = \dot{y} = 0 \quad \text{at} \quad t = 0$$

$\omega_t$  being given by eqn. (11). The solution depends upon the difference between  $\omega$ , the frequency of stimulation, and  $\omega_t$ , the frequency of free vibration of the filter. If the frequencies are approximately equal, and  $Q'$  is large, in eqn. (13)  $y$  is given approximately by

$$y = A \{ \cos (\omega t + \phi') - e^{-\frac{1}{2}\gamma t} \cos (\omega_t t + \phi') \} \quad (\omega \simeq \omega_t) \quad (14)$$

and on stimulation at  $\omega_t$ ,

$$y = A \cos(\omega_t t + \phi') \{1 - e^{-\frac{1}{2}\gamma t}\} \quad (\omega = \omega_t). \quad (15)$$

Eqns. (15) and (10), which describe the build up and decay of the response of a linear second-order filter to a short sinusoidal input at angular frequency  $\omega_t$ , have been used to fit the hair cell's response to tone bursts at the c.f.; since the output,  $y$ , is a voltage,  $A$  must include the sensitivity constant,  $S$  at the c.f., and also  $p$ , the sound pressure.

$$A = \sqrt{2}.p.S. \quad (16)$$

Fig. 16*A* shows an averaged linear response to a tone burst of duration 43 msec at 276 Hz, 55 db s.p.l. for the hair cell of Fig. 8. The squares are theoretical values calculated from eqns (10), (15) and (16), with  $\omega/2\pi = 276$  Hz,  $\omega_t/2\pi = 271$  Hz,  $\gamma = 1.781 \times 10^2 \text{ sec}^{-1}$ ,  $S = 88.8 \text{ mV/Pa}$  and  $\phi = \phi' = 41^\circ$  (the two phase angles are equal since the stimulus was an integral number of cycles). The quality factor  $Q'$ , calculated for the cell is 9.56. This is in reasonable agreement with the  $Q$  of 8.4 obtained directly from the linear iso-intensity curve for this cell (Fig. 17). A sensitivity constant can also be calculated from the linear iso-intensity curve; its value at the resonant frequency is 94.8 mV/Pa. The agreement between the values calculated in the two different ways provides some justification for the assumption that the cochlear filtering system behaves linearly for small inputs.

In fitting the responses to tone bursts, we have assumed that there is no delay between the start of the pressure wave at the tympanum and the input to the resonant system. This was justified by the finding that the latency to the start of the click response in this cell was a small fraction of a millisecond (see page 33), a delay which does not significantly affect the fit.

A complete fit to the responses to tone bursts was possible for two other hair cells, although in these cases, the difference between  $\omega$  and  $\omega_t$  was sufficiently large that eqn. (14) had to be used. Then the initial part of the response consisted of a beating between the free and forced vibrations. For these, and several other cells, eqn. (10) could be used to fit the decay of the oscillations at the termination of the tone burst, and hence to determine  $\omega_t$  and  $Q'$  for each of the cells. The results of these measurements are summarized in Table 4, which includes, for comparison, the values of these parameters derived from measurements of a linear iso-intensity tuning curve for each cell. For seven of the cells, the agreement between the two sets of values is good; for the other two cells, the  $Q$  value derived from measurements of tone bursts was significantly higher than that from the iso-intensity curve. This discrepancy may be related to the fact that, for both cells, the state of the recording was changing during the course of the frequency sweeps, and was associated with changes in the c.f. and the sharpness of tuning as described in the previous section.

*Responses to clicks.* Fig. 16*B* shows the averaged response of the hair cell of Fig. 16*A* to condensation clicks, each producing a pressure change of  $2 \times 10^{-4}$  Pa sec at the tympanum. Although the driving voltage delivered to the earphone had the form of an impulse, the wave form of the pressure change was a brief oscillation determined by a resonance in the earphone. The intensity of the click was obtained by integrating the wave form of the pressure change recorded by the condenser microphone and

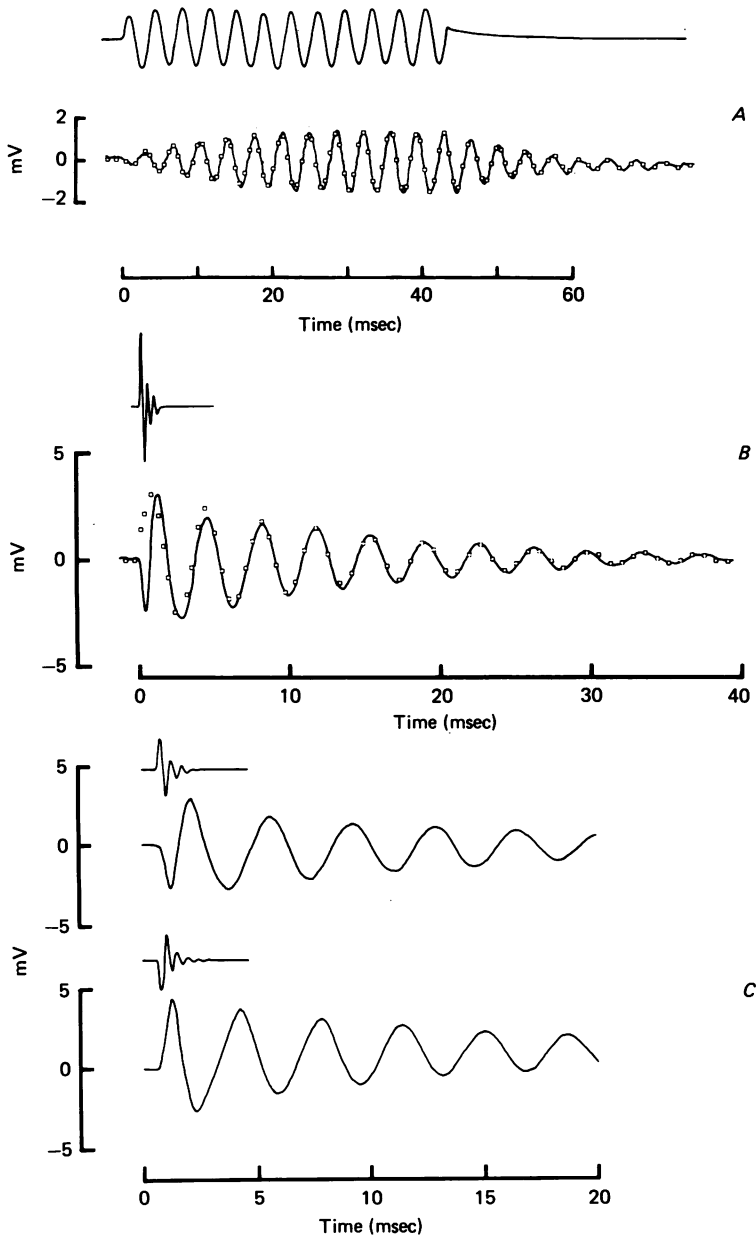


Fig. 16. Resonance phenomena in a hair cell. *A*, the averaged response to 128 tone bursts at 276 Hz, 55 db re  $20 \mu\text{Pa}$ . *B*, the averaged response to sixty-four compression clicks of intensity  $2 \times 10^{-4} \text{ Pa.s}$  for the same cell. *C*, averaged responses to compression (upper) and rarefaction clicks (lower) on an expanded time scale; same intensity as in *B*. Note the non-linearity in first cycle of response. The squares in *A* and *B* represent the theoretical behaviour of a linear single stage resonance filter, and have been calculated as described in the text, with a resonant frequency = 271 Hz,  $Q = 9.56$  in *A* and resonant frequency = 274 Hz,  $Q = 11.86$  in (*B*). Upper trace of each pair is the sound monitor, the oscillation in the sound pressure of the click at about 2 kHz is due to an earphone resonance. The form of the click is uncorrected for the probe tube, which also introduced a delay of about  $100 \mu\text{s}$ . Sound pressure at tympanum due to click thus starts slightly earlier than indicated. Characteristic frequency of cell, 274 Hz. Resting potential  $-54 \text{ mV}$ . Temp. =  $21.5^\circ \text{C}$ ; see Figs. 8 and 17 for other details of same cell.

probe tube. It was later checked that recording through the probe tube did not significantly alter the measured intensity of the click. Owing to conduction delay, the onset of the click recorded through the probe tube was delayed by about 100  $\mu$ sec relative to the pressure change at the tympanum.

Despite the resonance of the earphone, the pressure change is still brief compared

TABLE 4. Comparison of  $Q$  values from tuning curves and terminal oscillations to tone bursts

Tuning curve		Tone bursts		
c.f. (Hz)	$Q$	$\omega_i/2\pi$ (Hz)	$\tau$ (ms)	$Q'$
94	2.35	78	14.14	3.46
100	1.16	53	3.96	1.49
250	4.03	264	8.33	6.91
274	8.40	271	11.28	9.58
274	7.21	278	7.19	6.28
311	5.87	314	17.19	16.97*
		273	8.44	7.23*
346	3.22	360	5.70	6.44
425	5.31	422	13.26	4.32
431	6.13	438	16.05	8.33

c.f., characteristic frequency;  $Q = Q_{s,ab}$  calculated from linear iso-intensity curve using eqn. (4).  $\omega_i/2\pi$ ,  $\tau$  and  $Q'$  calculated from damped oscillations occurring at end of response to an un-tapered tone burst at a frequency close to c.f. of cell.  $\omega_i/2\pi$ , frequency of oscillations;  $\tau$ , time constant of decay of the amplitude of oscillations;  $Q'$  calculated from these two parameters using eqns. (11) and (12).

\* Two sets of values obtained at different times during recording.

with the period of the damped oscillation produced in the hair cell. The squares in Fig. 16B have been calculated from the impulse response of the second order resonance filter, given by

$$y = y_0 e^{-\frac{1}{2}\gamma t} \cos(\omega_1 t + \phi''), \quad (17)$$

with  $y_0 = 3.3$  mV,  $\omega_1/2\pi = 274$  Hz,  $\gamma = 1.449 \times 10^2$  sec $^{-1}$ ,  $\phi'' = -79^\circ$ . The response shown was at the lowest intensity used for this cell, and although the maximum peak-to-peak voltage is only 6 mV, the initial part of the response is clearly non-linear, the non-linearity of the first two cycles being emphasized by the asymmetry between the condensation and rarefaction click responses (Fig. 16C). The later part of the response, however, is an exponentially decaying oscillation at the c.f. of the cell, and is fitted well by eqn. (17). From the parameters used to achieve the fit, a  $Q'$  of 11.86 was calculated for the filter.

The sensitivity  $S$  of the cell at its c.f., can also be inferred from the value used to fit the click response. For the second order resonance,  $S$  is given (for large  $Q'$ ) by

$$S = \frac{y_0 Q'}{p \Delta t \omega_0} \quad (18)$$

$p \Delta t$  is the pressure change in the click and is  $2 \times 10^{-4}$  Pa sec. Using the appropriate values for the other constants, a sensitivity of 113.7 mV/Pa can be calculated. The difference between this sensitivity and that obtained from the fit to the tone bursts



is accounted for almost entirely by the higher value of  $Q'$  required for fitting the click response.

We have not examined the click responses of other hair cells in any detail, but there are several features worth noting in the records of Fig. 16. First the response was very rapid, which is consistent with the results of Corey & Hudspeth (1979) who observed latencies of 40  $\mu$ sec or less to the microphonics in the frog sacculle. Following the click, the hair cell potential changed with a latency of a fraction of a millisecond and, from the initial polarity it can be seen that the cell depolarized to a rarefaction and hyperpolarized to a compression. A rarefaction should result in the basilar membrane moving towards the scala vestibuli, and, on the conventional scheme of hair cell excitation (ter Kuile, 1900; Wever, 1971) this would lead to a bending of the cilia of the hair cells in a direction away from the neural limb. Since each cell's ciliary bundle is polarized with its kinocilium placed abneurally (Miller, 1978), the cell of Fig. 16 would thus produce a depolarization on the bending of the cilia towards the kinocilium, and would hyperpolarize to ciliary deflections away from the kinocilium. This scheme for the polarity of the transduction is the same as that postulated for other hair cell systems (Lowenstein & Wersäll, 1959; Goldberg & Fernandez, 1971; Hudspeth & Corey, 1977).

In fitting the hair cell's responses to tone bursts and clicks, the phase of the theoretical sinusoid was adjusted arbitrarily to obtain the best fit to the data. However, for the second order resonance, the phase shift is not arbitrary. Thus in eqn. (15)  $\phi' = -90^\circ$  for stimulation at the resonant frequency. Experimentally the hair cell potential (Fig. 16A) was found to lag the sound at the tympanum by  $-62^\circ$ , provided depolarizations of the cell were referred to rarefactions, as is indicated by the initial polarity of the click responses. A more detailed discussion of the phase behaviour of the hair cell responses is postponed until a later paper (Crawford & Fettiplace, 1980).

*Shape of the tuning curve.* Since a single-stage resonance has been used to fit the responses to tone bursts and clicks, it was of interest to examine whether the shape of the hair cell tuning curve was consistent with such a resonance. The amplitude spectrum of the filter whose differential equation is eqn. (8) can be put in the following form:

$$A = \frac{\sqrt{2} \cdot S \cdot p \cdot \omega_0^2}{((\omega_0^2 - \omega^2)^2 Q^2 + \omega_0^2 \omega^2)^{\frac{1}{2}}}, \quad (19)$$

$2A$  is the peak-to-peak response as a function of the angular frequency  $\omega$ ,  $S$  is the sensitivity at the characteristic frequency and  $p$  is the sound pressure. Such a curve can be made to fit the central region of the linear tuning curve around the c.f. For the cell of Fig. 16, a fit was achieved over the upper 6 db of the curve with a  $Q$  of about 8.9. A better over-all fit to the tuning curve can however be achieved by a slightly modified equation:

$$A = \frac{\sqrt{2} \cdot S \cdot p \cdot \omega_0}{(1 + Q^2)^{\frac{1}{2}}} \left\{ \frac{\omega_0^2 + \omega^2 Q^2}{(\omega_0^2 - \omega^2)^2 Q^2 + \omega_0^2 \omega^2} \right\}^{\frac{1}{2}}. \quad (20)$$

This is the resonance spectrum, which can be derived to describe the modulus of the complex impedance of a combination of a resistance and inductance in parallel with a

capacitance (Donaldson, 1958). Fig. 17 shows a linear tuning curve obtained from a frequency sweep at an approximately constant intensity for the cell of Fig. 16. The sound pressure,  $p$ , was 51 db re  $20 \mu\text{Pa}$ , and the cell was generating a maximum response of about 2 mV (at the c.f.) which was in the linear range. The circles were calculated from eqn. (20) with  $Q = 8.4$ ,  $\omega_0/2\pi = 274 \text{ Hz}$  and  $S = 94.8 \text{ mV/Pa}$ ,

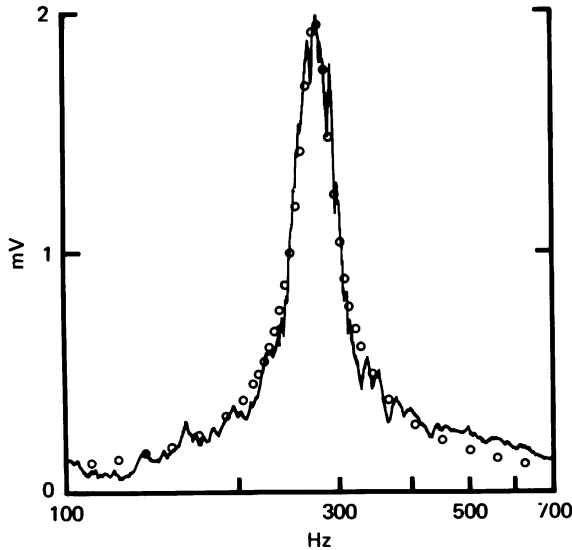


Fig. 17. Linear iso-intensity curve for hair cell of Fig. 16. The ordinate is the peak-to-peak amplitude of the sinusoidal response of the cell to a continuous tone whose frequency, plotted on the abscissa, was swept at an approximately constant intensity. The record, which was the output of the 'omniphase' was obtained with the two phase-lock amplifiers at a band width of 0.33 Hz, as described in the Methods. The circles give the form of the tuning for a parallel resonance, and were calculated from eqn. (20) in the text, with a resonant frequency = 274 Hz and  $Q = 8.4$ . Due to the frequency selectivity of the earphone, the sound pressure at the tympanum increased by about 3 db from 100 to 700 Hz, and at 274 Hz had a value of 51.3 db re  $20 \mu\text{Pa}$ ; the frequency was swept exponentially at a rate of about 1 decade per 20 sec. Characteristic frequency of cell, 274 Hz; maximum peak-to-peak response 35 mV, resting potential - 54 mV. Temp. 21.5 °C. Same cell as Figs. 8 and 16.

the agreement with the experimental curve being good. We would conclude that the shape of the central region of the hair cell's tuning curve, as well as the small responses to transient stimuli, can be well fitted by a theory incorporating a single-stage resonance.

#### *Random fluctuation in the hair cell potential*

Recordings from hair cells with large responses were characteristically very noisy, and in the absence of deliberate sound stimulation the voltage fluctuated in an apparently random manner with an amplitude of about 5–10 mV peak-to-peak. A striking property of the noise is illustrated in Fig. 18 which gives segments of voltage records from six different cells. It may be seen that the major frequency components in the fluctuations differ from cell to cell and appear to correlate

with the c.f. of the cell, which is given beside each trace. Thus, for example, the noise in the 425 Hz cell clearly contains higher frequency components than those from either the 94 Hz or 100 Hz cells. To examine the point more quantitatively, we measured the spectrum of the noise in the hair cell voltage as described in the Methods; in

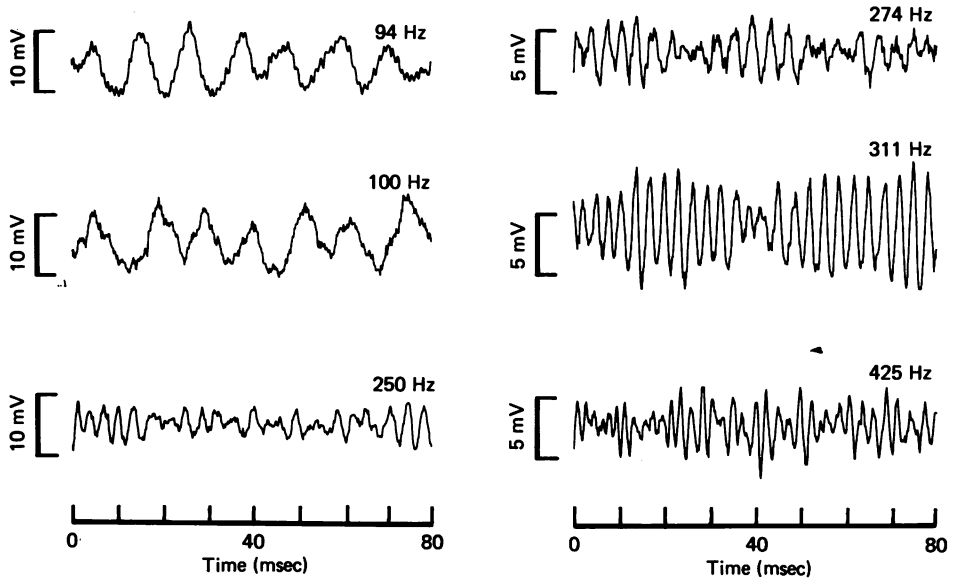


Fig. 18. Voltage fluctuations in the recordings from six different hair cells in the absence of deliberate sound stimulation. The c.f. of the cell is given beside each trace. (Note that the major frequency components in the fluctuations are correlated with the c.f. of the cell.) The conditions of recordings and tuning properties of the cells are given in Table 1, and the properties of the voltage noise are presented in Table 5.

TABLE 5. Characteristics of hair cell voltage noise

c.f. (Hz)	$V_i$ ( $\mu\text{V}/\sqrt{\text{Hz}}$ )	$V_o$ ( $\mu\text{V}/\sqrt{\text{Hz}}$ )	$V_n$ ( $\mu\text{V}/\sqrt{\text{Hz}}$ )	$S_n$ (mV/Pa)	$S$ (mV/Pa)	$S_n/S$ (db)
90	190.6	4.8	190.5	569	3.7	43.7
100	72.0	4.8	71.8	239	47.0	14.1
250	45.0	3.6	44.9	374	18.9	25.9
274	140.2	11.8	139.7	1270	85.6	23.4
311	40	4.1	39.8	410	41.9	19.8
346	46.4	3.6	46.3	526	67.2	17.9
425	16	2.2	15.9	224	16.3	22.8

c.f., characteristic frequency;  $V_i$ ,  $V_o$  voltage noise at c.f. with electrode inside and outside cell respectively;  $V_n$ , hair cell voltage noise given by  $V_n = (V_i^2 - V_o^2)^{1/2}$ ;  $S_n$ , apparent noise sensitivity calculated from  $V_n$  and intensity of room noise at c.f.;  $S$ , linear sensitivity derived from tone presentations.

addition, a spectrum of the noise due to the electrode alone was obtained using a stretch of record with the electrode just outside the cell. This came from the end of the experiment and it is assumed that there was no change in the electrode properties on loss of the penetration.

The results of these measurements on one cell are shown in Fig. 19A which gives

the spectra of the r.m.s. noise voltage with the electrode inside (filled circles) and outside (open circles) the cell. Most of the power in the hair cell noise was concentrated in a narrow band of frequencies around the c.f. of the cell (274 Hz) with the peak occurring at 280 Hz. In contrast, the electrode noise was virtually flat up to about 1 kHz, and was a factor of twelve smaller than the hair cell noise at the c.f. of cell. The total variance in the hair cell noise for the frequency band 190 to 350 Hz was  $1.1 \text{ mV}^2$ . Similar results were obtained from the noise spectra of other cells. Thus, for example, the cell with a c.f. of 94 Hz had a peak noise voltage at 85 Hz, and the cell with a c.f. of 425 Hz had a peak noise voltage at 450 Hz. In each case the value at the peak was about an order of magnitude larger than the electrode noise alone. Peak noise voltages and the corresponding values corrected for the noise in the electrode are presented in Table 5 for seven cells. The conclusion from these results is that, whatever the origin of the noise, it is present in the hair cell potential during a recording and is correlated with the tuning properties of the cell.

*Cross correlation between hair cell noise voltage and acoustic noise pressure*

An obvious possible source of the noise voltage in the hair cells is background acoustic noise present at the tympanum. A difficulty immediately arises, however, if this explanation is pursued quantitatively; by measuring the standard deviation of the hair cell noise voltage and the standard deviation of the acoustic noise pressure over the same band of frequencies as those present in the hair cell signal, one can calculate a sensitivity constant in  $\text{mV}/\text{Pa}$ . This calculation assumes linearity but the magnitude of the hair cell voltage fluctuations lies close to the range over which the cells responded linearly to intentionally presented sounds. Thus in the example shown in Fig. 19A the hair cell produced a voltage noise signal of  $139.7 \mu\text{V}/\sqrt{\text{Hz}}$  at 280 Hz. At the same frequency the acoustic noise at the tympanum had a value of  $1.1 \times 10^{-4} \text{ Pa}/\sqrt{\text{Hz}}$  (about four times the equivalent pressure noise level in the microphone preamplifier) and hence the apparent sensitivity of the cell was  $1270 \text{ mV}/\text{Pa}$ . In comparison, the cell's sensitivity to tones of the same frequency was  $86 \text{ mV}/\text{Pa}$ . Further examples of this calculation are given in Table 5. Considered in this way, all hair cells are apparently about an order of magnitude more sensitive to the background acoustic noise than they are to tones presented at the c.f. of the hair cell. This large discrepancy led us to suspect that the hair cell voltage noise arose by a process other than spurious acoustic stimulation. One direct check is to examine the cross correlation function between the two noise signals; if hair cells act as independent noise generators then the voltage fluctuations in the cell will be completely uncorrelated with the pressure fluctuations at the tympanum.

The filled circles in Fig. 19B are an example of the cross-correlation coefficient (eqn. (2)) between acoustic and hair cell voltage noise for the cell of Fig. 19A in the absence of intentional stimulation. These were calculated from sample records 26 s long and for lag times of 0.5–30 ms. The maximum value of the cross-correlation coefficient ( $\rho_{pV}$ ) was 0.005. Since the standard deviation of the correlation calculated using eqn. (3) was 0.005, the samples contain no significant cross-correlated components. To check the accuracy of the correlation, a tone at 60 db s.p.l. and 263 Hz was presented and the cross-correlation coefficients calculated from samples of hair cell voltage and tympanic pressure of duration 0.256 s. These conditions of stimula-

tion produced a signal in the hair cell whose variance was  $3.055 \text{ mV}^2$  when the variance in the absence of the tone was  $2.697 \text{ mV}^2$ . The peak-to-peak response to the tone is thus comparable to the peak-to-peak amplitude of the voltage fluctuations. If the transduction is linear the cross-correlation function ( $R_{pV}$ ) should have the form

$$R_{pV}(\tau) = \frac{\bar{V}\bar{P}}{2} \cos(\omega\tau + \theta), \quad (21)$$

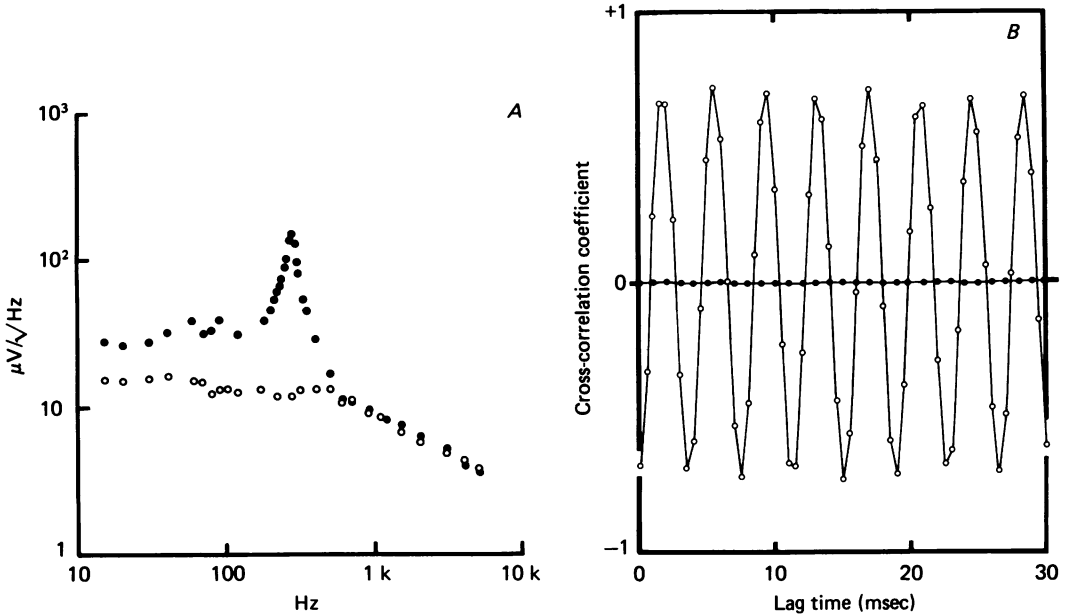


Fig. 19. Spectra for the voltage noise in a hair cell recording. *A*, r.m.s. voltage plotted against frequency for electrode inside the cell (●) and outside the cell (○). Analysis performed on stretches of record about 1 min in duration; no sound was being presented during the course of the recording. Stretch of record with electrode outside cell was obtained immediately after loss of penetration. *B*, cross-correlation between the hair cell voltage noise and the sound pressure at the tympanum. Ordinate: cross-correlation coefficient (see Methods); abscissa: lag of the hair cell voltage with respect to the sound pressure (similar results were obtained with negative lags). ●, no deliberate acoustic stimulation; length of record analysed, 26 s; voltage variance  $2.690 \text{ mV}^2$ . ○, continuous tone at 263 Hz, 60 db s.p.l.; length of record 256 ms; voltage variance  $3.055 \text{ mV}^2$ . Same cell as Fig. 19*A*. The maximum standard deviation of the correlation coefficient was 0.005 (filled circles) and 0.057 (open circles).

where the stimulating tone has the form  $\bar{P} \cos \omega t$ , the hair cell response the form  $V(t) = \bar{V} \cos(\omega t + \theta)$  and  $\tau$  is the lag time. Expressed as a cross correlation coefficient,  $\rho_{pV}$  (see Methods), this has the form

$$\rho_{pV}(\tau) = \cos(\omega\tau + \theta) \quad (22)$$

and assumes values between +1 and -1. The correlogram shown in Fig. 19*B* (open circles) has a frequency of 263 Hz and mean maximum values of  $\rho_{pV}$  of  $\pm 0.67$ . Thus tonal stimuli that produce voltage responses in the hair cell quite modest compared with the amplitude of the spontaneous voltage fluctuations show clear cross-correlation with the pressure at the tympanum.

It might be thought that  $\rho_{pV}$  should assume maximum values of  $\pm 1$  for tonal stimulation: this is not so if hair cell signals contain an independent uncorrelated component as is clearly the case. If the hair cell voltage has a total variance  $\sigma_T^2$  comprising a sinusoidal component at the stimulating frequency of variance  $\sigma_s^2$  and an uncorrelated noise component of variance  $\sigma_n^2$  then

$$\sigma_T^2 = \sigma_n^2 + \sigma_s^2 \quad (23)$$

and

$$\sigma_s^2 = \rho_{\max}^2 \sigma_T^2 \quad (24)$$

where  $\rho_{\max}$  is the maximum value of the correlation coefficient. For the example illustrated in Fig. 19B where  $\sigma_T^2$  was 3.055 mV<sup>2</sup> and  $\rho_{\max}$  was 0.67  $\sigma_s^2$  would be 1.371 mV<sup>2</sup> and the peak-to-peak amplitude of the sine wave response would be 3.31 mV. This value compares well with the value of 3.37 mV obtained by averaging. Similarly the value of  $\rho_n^2$ , the uncorrelated component, would be 1.68 mV<sup>2</sup> which is in reasonable agreement with the value of the noise variance obtained in the absence of the stimulating tone.

A more extreme example of the depression of  $\rho_{pV}$  by the uncorrelated hair cell noise was obtained for this cell by presenting a tone at 40 db s.p.l. and 263 Hz. This gave values of  $\rho_{\max}$  of 0.0607 with a value of 2.998 mV<sup>2</sup> for  $\sigma_s^2$ . The response to the tone therefore had a variance of 0.011 mV<sup>2</sup> and a peak-to-peak amplitude of 0.297 mV. This value is again in agreement with the averaged value of the hair cell response which behaves linearly at these sound pressures (reducing the sound pressure by a factor of ten reduced the response by a factor of eleven as assessed from the cross-correlation methods).

The calculation of apparent sensitivity to the background acoustic noise is therefore grossly misleading because the hair cell voltage noise arises by a process independent of acoustic stimuli. We can calculate the maximum expected correlation coefficient in the absence of deliberate stimulation using the acoustic sensitivity constant of the cell obtained from tonal stimulation (86 mV/Pa), and the acoustic noise pressure. Assuming that all the correlated power lies in a 1 Hz band at the c.f. (which is a very generous estimate) the standard deviation of the true noise correlogram would be 0.0095 mV when the background acoustic noise in a 1 Hz band at the c.f. (274 Hz) was  $1.1 \times 10^{-4}$  Pa. This would yield a value for  $\rho_{\max}$  of 0.006, which is comparable to the standard deviation of the measurement (0.005).

#### *Periodicity in the spontaneous firing of auditory nerve fibres*

One question of interest is whether the voltage fluctuations seen in the hair cells manifest themselves in the basal discharge of the auditory nerve fibres. Since our measurements of hair cell sensitivity indicate that at sound pressures which correspond to the threshold at the c.f. of the auditory nerve fibres, the hair cells produce signals about 1 mV in amplitude and the hair cell voltage noise signals are at least comparable to this, we would expect to find evidence of the existence of the voltage fluctuations in the auditory nerve firing. The question is of more than corroborative interest since it seems quite possible that the presence of the micro-electrode in the cochlear partition might exaggerate or otherwise modify the hair cell voltage fluctuations.

Inter-spike interval histograms were compiled of the spontaneous discharge of forty auditory nerve fibres in five preparations. Two examples are shown in Fig. 20. Rates of discharge varied from a few impulses/sec to 72 impulses/sec, but due to the need for large numbers of spikes to construct a histogram, only those fibres with discharge rates greater than 10 impulses/sec were investigated in detail. To this extent the sample is biased. Of the forty fibres examined, thirty-three showed a

clear periodicity in the interval histogram, which in extreme cases (see Fig. 20A) consisted of a series of equally spaced peaks whose amplitude declined approximately exponentially with time interval. A more typical example, however, is shown in Fig. 20B, in which the periodicity in the histogram is less pronounced. These histograms differ from histograms of spontaneous activity in mammalian auditory nerve fibres (Kiang *et al.* 1965; Walsh, Miller, Gacek & Kiang, 1972) which show no evi-

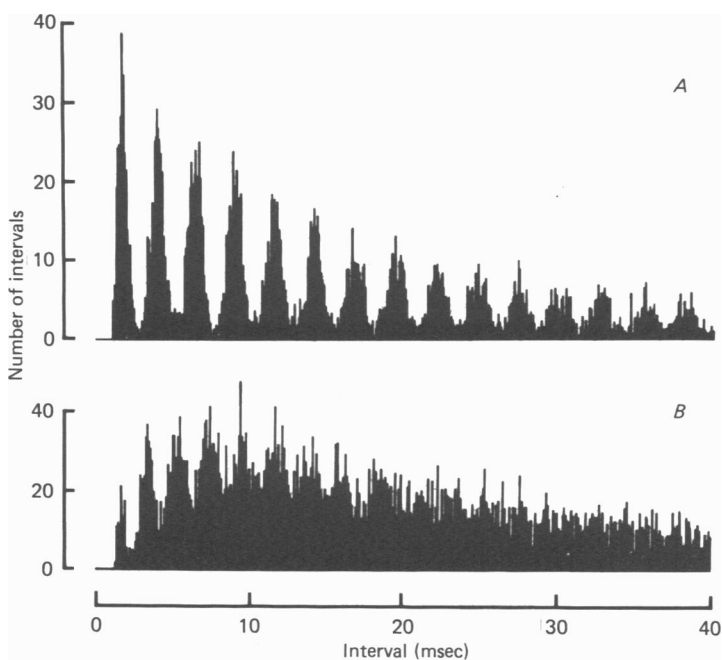


Fig. 20. Interspike interval histograms for the spontaneous firing in two auditory nerve fibres in the absence of deliberate acoustic stimulation. *A*, characteristic frequency 380 Hz, threshold at c.f. 43.5 db s.p.l., spontaneous firing 43 spikes/sec. *B*, characteristic frequency 480 Hz, threshold at c.f. 44.6 db s.p.l., spontaneous firing 33 spikes/sec. Histograms consist of 500 bins each of 80  $\mu$ sec duration. In each histogram, note the periodicity which correlates with the c.f. of the fibre.

dence of periodicity. The intervals between successive peaks in the histogram coincided, in all thirty-three fibres, with the reciprocal of the characteristic frequency of the fibre. The periodicity is what one would expect as a result of the hair cell voltage fluctuations as these occupy a narrow frequency band centred on the characteristic frequency of the hair cell. A more quantitative comparison is rendered difficult however, because it is not known how many hair cells converge synaptically on to a single auditory nerve fibre in the turtle, nor is it clear how the probabilistic nature of the synaptic transmission process will affect the firing. However it does seem that the presence of the electrode in the cochlear partition is not a requirement for the generation of the hair cell voltage noise.

A similar periodicity, whose preferred interval was inversely related to the c.f. of the cell, has been observed by Manley (1979) for the spontaneous firing of auditory nerve fibres in the gecko and the starling. He reported that the periodicity was present even though the experiments were performed in a sound-attenuation

chamber, which argues against the phenomenon arising by inadvertent stimulation due to extraneous noise.

In two experiments the tympanum was completely removed and the columella clipped back close to the quadrate bone. Auditory nerve fibre thresholds in these

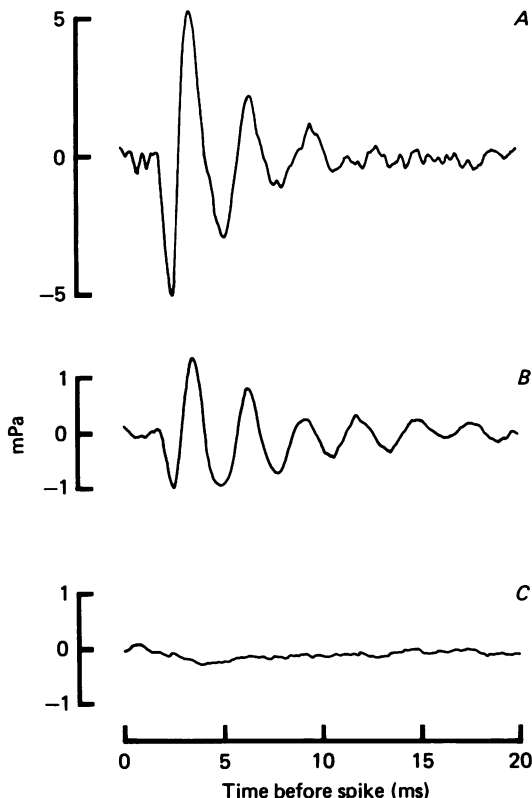


Fig. 21. Reverse correlograms between the spikes in a nerve fibre and the sound pressure at the tympanum: in the absence of deliberate acoustic stimulation (*C*) and in the presence of added acoustic noise at 66 db s.p.l. (*B*) and 76 db s.p.l. (*A*). Each record represents the average sound pressure for 20 ms before the occurrence of a spike which takes place at time zero (see Methods for details of measurement). The mean firing rate was 43 spikes/s (*C*), 58 spikes/s (*B*) and 76 spikes/s (*A*); same cell as Fig. 20*A*. Number of sweeps to produce average: *A*, 1024; *B*, 4096; *C*, 2048.

animals were  $86.3 \pm 9.4$  db s.p.l. (mean  $\pm$  s.d.;  $n = 16$ ) and  $99.0 \pm 8.1$  db s.p.l. (mean  $\pm$  s.d.;  $n = 15$ ). These values represent a sensitivity loss of about 40 db which is similar to the loss in sensitivity as assayed by the cochlear microphonic in *Pseudemys* on removal of the tympanum (Wever & Vernon, 1956). Despite the loss in sensitivity, high spontaneous firing rates were still observed. Interval histograms of the spontaneous firing were examined in twenty nerve fibres in these animals and seventeen showed clear evidence of periodicity. In view of the grossly impaired sensitivity of the ear under these conditions it seems unlikely that background acoustic stimulation could contribute significantly to the existence of the periodic discharge in the auditory nerve of the turtle.



The histograms shown in Fig. 20 bear many resemblances to interval histograms obtained by Rose, Brugge, Anderson & Hind (1967) from squirrel monkey auditory nerve fibres when stimulated with continuous tones at the c.f. of the fibre. As a further check on the lack of effect of spurious acoustic stimulation in our experiments we used the technique of triggered correlation (de Boer, 1968; de Boer & Kuyper, 1968) to look for a correlation between the spontaneous auditory nerve discharge and the sound pressure at the tympanum. The procedure reveals any consistent features of the sound pressure wave form that precede the occurrence of a spike in the auditory nerve. Since the hair cell voltage fluctuations are uncorrelated with the background acoustic fluctuations we would expect the triggered correlograms to confirm this point. Fig. 21 shows triggered correlograms for a nerve fibre whose interval histogram is shown in Fig. 20*A*. The fibre had a spontaneous firing rate of 43 spikes/s with a particularly pronounced periodicity. On deliberately adding in acoustic noise at 66 db s.p.l. the mean firing rate increased to 58 spikes/s and with the added noise at 76 db s.p.l. the mean firing rate was 76 spikes/s. The triggered correlograms obtained under these conditions are shown in Fig. 21 *A* and *B*. Both correlograms show a damped oscillation at about 380 Hz, which was the c.f. of the fibre. The similarity between the wave forms and the hair cell click response is striking (see Fig. 16) and interestingly, correlograms begin with a negative pressure deflection indicating again that the rarefaction phase of the sound is excitatory. In contrast to these correlograms, that obtained from the spontaneous discharge in the absence of intentional acoustic stimulation was flat (Fig. 21 *C*). This was the case in all of the thirty-three fibres that were examined, no matter how many sweeps were averaged. These results provide further support for the idea that most of the spontaneous firing in the auditory nerve is not a consequence of spurious acoustic stimulation of the ear.

#### DISCUSSION

##### *The isolated cochlea*

We have used an isolated cochlea preparation in the hope that its mechanical stability would improve the chances of making intracellular recordings from the hair cells. The viability of the isolated preparation is indicated by the sensitivities and sharp tuning curves of the auditory nerve fibres, and its suitability for this kind of experiment is confirmed by the large voltage responses that can be recorded intracellularly from the hair cells. These potentials are larger than previous measurements made in the reptilian cochlea (Mulroy *et al.* 1974) but are comparable to responses reported for inner hair cells in the guinea-pig cochlea (Russell & Sellick, 1978). The survival of the isolated reptilian preparation was first described by Adrian *et al.* (1938), who recorded auditory responses in the tortoise and the alligator. The relative immunity to anoxia of the turtle cochlea is remarkable in comparison to the mammal, where merely slowing the rate of artificial ventilation has been shown to detune and increase the thresholds of the auditory nerve fibres (Robertson & Manley, 1974). Some of this difference may be a consequence of the susceptibility to anoxia of the endocochlear potential in the mammal unlike the turtle (Schmidt & Fernández, 1962). However, the ability of the turtle to survive on anaerobic metabolism associated with its prolonged diving (Robin, Vester, Murdaugh

& Millen, 1964) is probably the major reason for the survival of the isolated preparation.

The lowest thresholds reported in this paper for the auditory nerve fibre responses were around 35–45 db s.p.l. The values are almost identical to the thresholds obtained by Paton, Moffat & Capranica (1976) for auditory nerve fibres in intact anaesthetized *Pseudemys*, and are similar to the auditory thresholds given by Manley (1970) for cells in the cochlear nucleus of the box turtle, *Terrapene carolina*. The nerve responses recorded by Adrian *et al.* (1938) were an order of magnitude less sensitive. The auditory range, reflected in the distribution of characteristic frequencies from about 30–700 Hz was also comparable to the range found in intact chelonia at room temperature, although Adrian *et al.* (1938) noted that the upper frequency limit of the nerve responses was temperature-sensitive, being reduced to about 200 Hz at 10 °C. The sensitivity of the middle ear transfer in *Pseudemys* has been found to fall off quite steeply above 650 Hz (Moffat & Capranica, 1978) which coincides with the upper limit of the distribution of c.f.s in the auditory nerve.

On the basis of these various comparisons we have no reason to believe that cochlear function in the most sensitive isolated preparations was seriously impaired. It is worth pointing out, however, that our results would indicate that the auditory sensitivity of the turtle over its optimal frequency range (200–600 Hz) is not as high as other reptiles such as the alligator, *Caiman crocodilus* (Klinke & Pause, 1977) or the alligator lizard *Gerrhonotus multicarinatus* (Weiss, Mulroy, Turner & Pike, 1976). Despite the difference in sensitivities, the sharpness of the tuning of the nerve fibres in all three reptiles is similar. The  $Q_{10\text{db}}$  values for the nerve fibre tuning in *Pseudemys* are two to three times larger than in the mammal over the same frequency range (for collected mammalian results see Evans, 1975).

#### *Nature of the resonance*

The detailed form of the responses and the tip of the tuning curve for several hair cells have been described by the equations for a single stage resonance. The most likely source of such a resonance would be in the mechanical properties of the basilar membrane. The rapid change in frequency with position may however present a difficulty in explaining the frequency selectivity of the turtle's cochlea solely in terms of the mechanics of the basilar membrane motion. This is illustrated by the following calculation. Assuming an exponential frequency map (eqn. (7)) then the 3 db bandwidth of a tuning curve is equivalent to a distance  $\Delta x$  along the basilar membrane given approximately (for large  $Q$ ) by

$$\Delta x = 2\lambda \log_e \left( 1 + \frac{1}{2Q_{3\text{db}}} \right), \quad (25)$$

where  $\lambda$  is the length of the basilar membrane over which there is an  $e$ -fold change in frequency. For  $\lambda = 135 \mu\text{m}$  (p. 106) and  $Q_{3\text{db}} = 10$ ,  $\Delta x$  is  $13.2 \mu\text{m}$  which is less than two hair cell diameters. Although a  $Q_{3\text{db}}$  of 10 corresponds to the most selective hair cell recorded from, some of the sharply tuned high frequency auditory nerve fibres had  $Q_{3\text{db}}$  values in the region of 20, which would give a  $\Delta x$  of  $6.6 \mu\text{m}$ . The diameter of a hair cell (about  $8 \mu\text{m}$ ) sets an upper limit on the sharpness of tuning

of a mechanical resonance on the basilar membrane that can be faithfully detected. For comparison the value of  $\lambda$  for the mammalian cochlea (von Békésy, 1960) is more than an order of magnitude larger than in the turtle, and so any tuning of the basilar membrane spans a much greater number of hair cells.

So far there have been no measurements of the basilar membrane motion in *Pseudemys* to confirm whether it is capable of performing a mechanical frequency analysis. The limitation on tuning imposed by the hair cell dimensions can be avoided by supposing either that the frequency selectivity is generated in more than one stage with the basilar membrane vibration not being as sharply tuned as the hair cell responses, or that the resonance could be entirely localized to the hair cell itself. In a subsequent paper (Crawford & Fettiplace, 1980) we will present evidence to support the idea that the major part of the frequency selectivity results from an electrical resonance in the hair cells.

An undesirable consequence of a sharply tuned resonance is the loss in time resolution for short tone bursts at the c.f. (Fig. 8). Since there is a scatter in the sharpness of tuning of auditory nerve fibres, however, there will be a concomitant variation in their temporal properties, and it is conceivable that this variation is part of a deliberate attempt to provide accurate coding of both the temporal and frequency characteristics of incoming signals. The time constant of the build up and decay of the linear responses is proportional to the 3 db bandwidth of the tuning curves which can vary from about 25 to 90 Hz thus producing a range of time constants from 3.5 to 12.7 ms.

#### *Hair cell sensitivity*

The sensitivity of the hair cells has been expressed in terms of the voltage they produce for a given sound pressure at the tympanum, the value for the most sensitive cell being about 90 mV/Pa. There are several steps which lie between the movements of the tympanum and the bending of the hair cell cilia, and it would be useful to derive a more direct measure of the sensitivity of the hair cell transduction mechanism. The only measurements of basilar membrane motion available for a reptile with a similar cochlea have been made in the alligator lizard (Weiss, Peake, Ling & Holton, 1978). These measurements extrapolate, on the assumption of linearity, to give a peak basilar membrane displacement of  $\pm 0.2$  nm at 40 db s.p.l. If one allows for a 20 db difference in auditory nerve fibre thresholds between the two species (making the assumption that all this difference derives from the lower sensitivity of the middle ear, there is evidence to support the view that at least 10 db can be accounted for in this way: e.g. Moffat & Capranica 1978) the basilar membrane displacement in the turtle might be closer to  $\pm 0.02$  nm at 40 db s.p.l. At this sound pressure, corresponding approximately to the animal's behavioural threshold (Fig. 4) the most sensitive hair cell would have been producing a maximum peak-to-peak response of 0.5 mV. This would therefore give a sensitivity of 12.5 mV per nm displacement of the basilar membrane.

To proceed any further it is necessary to make an assumption about what is the effective stimulus for hair cell excitation. For example, stimulation could be determined by the angle of deflexion of rigid cilia pivoted at the point at which they are joined to the apical surface of the cell. An alternative assumption would be that

excitation is a consequence of a shearing force between the hair cell body and the cilia which are embedded in the tectorial membrane (ter Kuile, 1900; von Békésy, 1960). Hudspeth & Corey (1977) have shown that saccular hair cells can be artificially stimulated by deflexion of their ciliary bundles with a glass probe slipped over the tips of the cilia. These results would be consistent with either of the excitation hypotheses, and, depending upon which is correct, there could be a considerable amplification of the transmitted force or angular deflexion (ter Kuile, 1900; von Békésy, 1960).

On the first hypothesis, if the cilia are assumed to be rigid and anchored only at their tips, the angle of deflexion of the basilar membrane from the horizontal is amplified by a factor approximately equal to the height of the basilar papilla (from the apical surface of the hair cell to the base of the membrane) divided by the length of the cilia. In the turtle this factor is about ten (see Pl. 2). Thus the hair cell sensitivity expressed in terms of the voltage response for a given angular deflexion of the cilia would have a value in the most sensitive cell of 2 V/degree. This is nearly three orders of magnitude greater than the 3 mV/degree inferred from the data of Hudspeth & Corey (1977) for the sensitivity of saccular hair cells. It is conceivable that the large discrepancy between the two values is due to the fact that the shearing force rather than ciliary deflexion is the effective stimulus for hair cell excitation. There may also be an amplification of the voltage signals introduced by the electrical resonance in the hair cells (Crawford & Fettiplace, 1980).

#### *Voltage noise in the hair cells*

The presence of voltage fluctuations in the hair cells in the absence of acoustic stimulation is an observation that finds parallels in recordings from statocyst hair cells of invertebrates (Detwiler & Fuortes, 1975; Wiederhold, 1978; DeFelice & Alkon, 1977). Statocyst hair cells show a spontaneous noise voltage when the statoconia lie over the sensory hairs. If the cyst is rotated so that the beat of the cilia is unhindered by the statoconia, the noise voltage disappears (Wiederhold, 1978; Grossman, Alkon & Heldman, 1979). It is possible that the noise signals in the cochlear hair cells of *Pseudemys* may have a similar origin for the ciliary bundles are restrained in pockets in the tectorial membrane. It would be envisaged that the cilia are motile, and that the voltage noise would arise due to restriction of their movement. There is, however, no evidence as yet to indicate that the cilia of the cochlear hair cells are motile.

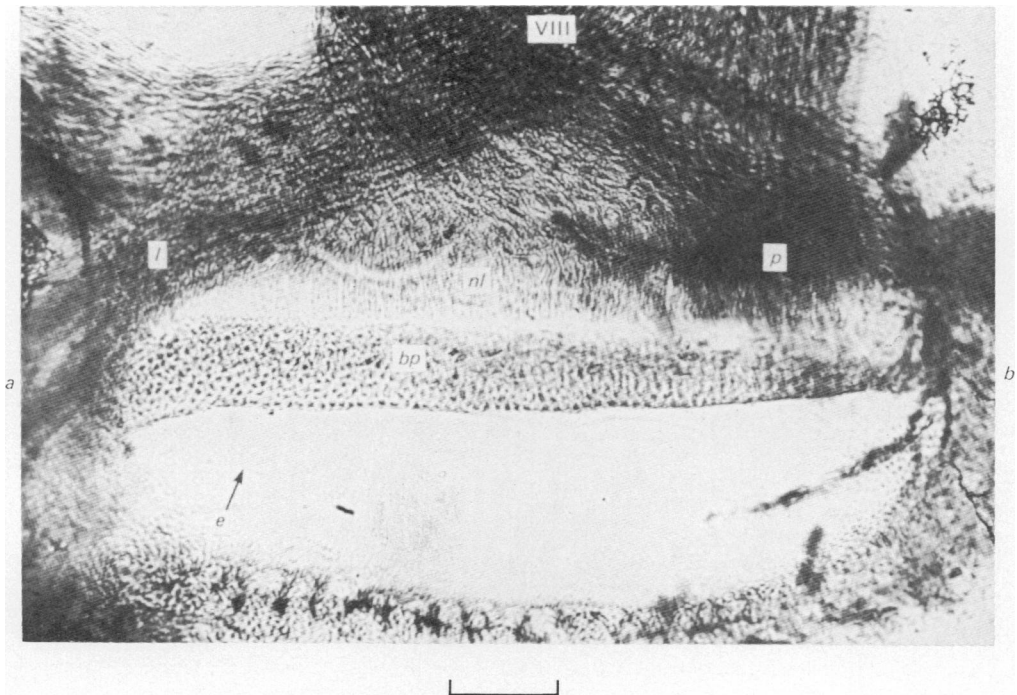
Since the spectrum of the noise voltage is comparable to the hair cell's tuning curve, this would argue that wherever the noise source is located, it precedes or is associated with the mechanism responsible for most of the hair cell's tuning. The presence of the noise poses a considerable problem for the animal in terms of signal detection since, in a given hair cell, it possesses the same frequency components and is several times larger in amplitude than the sound-induced voltages at the behavioural threshold. There is, however, an interaction between the noise voltage and the sound-induced voltages. For the largest responses the noise is completely suppressed, but the noise variance may be somewhat reduced even in the presence of smaller responses.

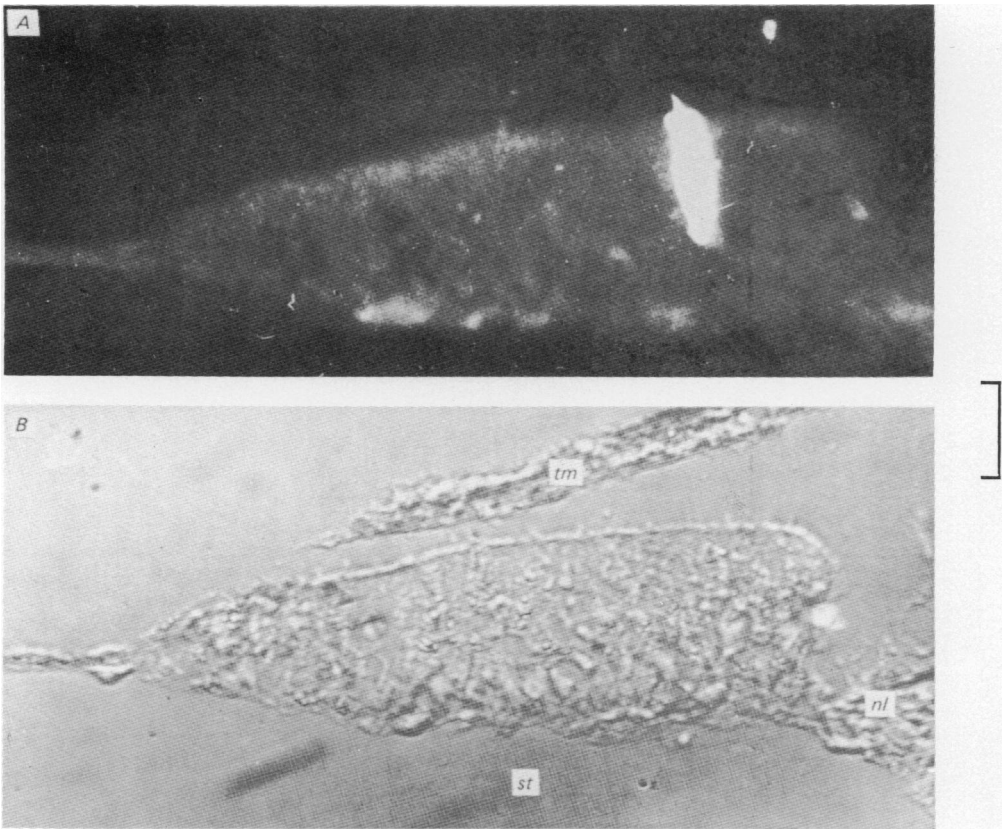
We are indebted to Mr P. L. Joyce and staff for building electronic equipment and Mr F. R. Lemmon for help with the histology. We also wish to thank Dr J. G. Robson for many helpful discussions and Professor A. L. Hodgkin, Professor A. F. Huxley and Dr T. D. Lamb for commenting on the manuscript. Dr W. W. Stewart kindly supplied us with a sample of the Lucifer yellow dye. We acknowledge the support of the Medical Research Council and a grant from the Elmore Trust to R. F.

## REFERENCES

- ADRIAN, E. D. (1931). The microphonic action of the cochlea: an interpretation of Wever and Bray's experiments. *J. Physiol.* **71**, 28–29P.
- ADRIAN, E. D., CRAIK, K. J. W. & STURDY, R. S. (1938). The electrical response of the auditory mechanism in cold-blooded vertebrates. *Proc. R. Soc. B* **125**, 435–455.
- BAIRD, I. L. (1960). A survey of the periotic labyrinth in some representative recent reptiles. *Univ. Kans. Sci. Bull.* **41**, 891–981.
- BAIRD, I. L. (1974). Anatomical features of the inner ear in submammalian vertebrates. In *Handbook of Sensory Physiology*, vol. V/1., ed. KEIDEL, W. D. & NEFF, W. D., pp. 159–212. New York: Springer Verlag.
- BAYLOR, D. A., FUORTES, M. G. F. & O'BRYAN, P. M. (1971). Receptive fields of cones in the retina of the turtle. *J. Physiol.* **214**, 265–294.
- BENDAT, J. S. & PIERSOL, A. G. (1971). *Random Data: Analysis and Measurement Procedures*. New York & London: John Wiley.
- COLBURN, T. R. & SCHWARTZ, E. A. (1972). Linear voltage control of current passed through a micropipette with variable resistance. *Med. Biol. Eng.* **10**, 504–509.
- COREY, D. P. & HUDSPETH, A. J. (1979). Response latency of vertebrate hair cells. *Biophys. J.* **26**, 499–506.
- CRAWFORD, A. C. & FETTIPLACE, R. (1978). Ringing responses in cochlear hair cells. *J. Physiol.* **284**, 120–122P.
- CRAWFORD, A. C. & FETTIPLACE, R. (1980). An electrical tuning mechanism in turtle cochlear hair cells. *J. Physiol.* (To be submitted.)
- DALLOS, P. (1973). *The Auditory Periphery: Biophysics and Physiology*. New York & London: Academic Press.
- DE BOER, E. (1968). Reverse correlation. I. A heuristic introduction to the technique of triggered correlation, with applications to the analysis of compound systems. *Proc. K. ned. Akad. Wet.* **71**, 472–486.
- DE BOER, E. & KUYPER, P. (1968). Triggered correlation. *IEEE Trans bio-med. Eng.* **15**, 169–179.
- DEFELICE, L. J. & ALKON, D. L. (1977). Voltage noise from hair cells during mechanical stimulation. *Nature, Lond.* **269**, 613–615.
- DESSAUER, H. C. (1970). Blood chemistry of reptiles – physiological and evolutionary aspects. In *Biology of the Reptilia*, vol. 3, ed. GANS, C., pp. 1–72. London & New York: Academic Press.
- DETWILER, P. B. & FOURTES, M. G. F. (1975). Responses of hair cells in the statocyst of *Hermisenda*. *J. Physiol.* **251**, 107–129.
- DONALDSON, P. E. K. (1958). *Electronic Apparatus for Biological Research*. London: Butterworths.
- EISENBERG, R. S. & JOHNSON, E. A. (1970). Three dimensional electric field problems in physiology. *Prog. Biophys. mol. Biol.* **20**, 1–65.
- EVANS, E. F. (1975). Cochlear nerve and cochlear nucleus. In *Handbook of Sensory Physiology*, vol. V/2, ed. KEIDEL, W. D. & NEFF, W. D., pp. 1–108. Berlin, Heidelberg & New York: Springer Verlag.
- FATT, P. & KATZ, B. (1952). Spontaneous subthreshold activity at motor nerve endings. *J. Physiol.* **117**, 109–128.
- FETTIPLACE, R. & CRAWFORD, A. C. (1978). The coding of sound pressure and frequency in cochlear hair cells of the terrapin. *Proc. R. Soc. B* **203**, 209–218.
- FURUKAWA, T. & MATSUURA, S. (1978). Adaptive rundown of excitatory post-synaptic potentials at synapses between hair cells and eighth nerve fibres in the goldfish. *J. Physiol.* **276**, 193–209.
- GARDNER, F. M. (1966). *Phaselock Techniques*. New York, London & Sydney: J. Wiley.

- GOLDBERG, J. M. & FERNÁNDEZ, C. (1971). Physiology of peripheral neurons innervating semi-circular canals of the squirrel monkey. I. Resting discharge and response to constant angular accelerations. *J. Neurophysiol.* **34**, 635-660.
- GROSSMAN, Y., ALKON, D. L. & HELDMAN, E. (1979). A common origin of voltage noise and generator potentials in statocyst hair cells. *J. gen. Physiol.* **73**, 23-48.
- HUDSPETH, A. J. & COREY, D. P. (1977). Sensitivity polarity and conductance change in the response of vertebrate hair cells to controlled mechanical stimuli. *Proc. natn. Acad. Sci. U.S.A.* **74**, 2407-2411.
- KIANG, N. Y. S., WATANABE, T., THOMAS, E. C. & CLARK, L. F. (1965). Discharge patterns of single fibres in the cat's auditory nerve. *M.I.T. Res. Mon.* **35**.
- KLINKE, R. & PAUSE, M. (1977). The performance of a primitive hearing organ of the cochlear type Primary fibre studies in the Caiman. In *Psychophysics and Physiology of Hearing*, ed. EVANS, E. F. & WILSON, J. P., pp. 101-111. London: Academic Press.
- LOWENSTEIN, O. & WERSÄLL, J. (1959). A functional interpretation of the electronmicroscopic structure of sensory hairs in the cristae of the elasmobranch *Raja clavata* in terms of directional sensitivity. *Nature, Lond.* **184**, 1807-1808.
- MANLEY, G. A. (1970). Comparative studies of auditory physiology in reptiles. *Z. vergl. Physiol.* **67**, 363-381.
- MANLEY, G. A. (1979). Preferred intervals in the spontaneous activity of primary auditory neurons. *Naturwissenschaften* **66**, 582-584.
- MILLER, M. R. (1978). Scanning electron microscope studies of the papilla basilaris of some turtles and snakes. *Am. J. Anat.* **151**, 409-436.
- MOFFAT, A. J. M. & CAPRANICA, R. R. (1978). Middle ear sensitivity in anurans and reptiles measured by light scattering spectroscopy. *J. comp. Physiol.* **127**, 97-107.
- MULROY, M. J., ALTMANN, D. W., WEISS, T. F. & PEAKE, W. T. (1974). Intracellular electric responses to sound in a vertebrate cochlea. *Nature, Lond.* **249**, 482-485.
- PATON, J. A., MOFFAT, A. J. M. & CAPRANICA, R. R. (1976). Electrophysiological correlates of basilar membrane motion in the turtle. *J. acoust. Soc. Am.* **59**, (Suppl. 1) S46.
- PATTERSON, W. C. (1966). Hearing in the turtle. *J. aud. Res.* **6**, 453-464.
- ROBERTSON, D. & MANLEY, G. A. (1974). Manipulation of frequency analysis in the cochlear ganglion of the guinea-pig. *J. comp. Physiol.* **91**, 363-375.
- ROBIN, E. D., VESTER, J. W., MURDAUGH, H. V. & MILLEN, J. E. (1964). Prolonged anaerobiosis in a vertebrate: anaerobic metabolism in the freshwater turtle. *J. cell. comp. Physiol.* **63**, 287-297.
- ROSE, J. E. (1970). Discharge of single fibres in the mammalian auditory nerve. In *Frequency Analysis and Periodicity Detection in Hearing*. eds. PLOMP, R. & SMOORENBURG, G. F., pp. 176-188. Leiden: A. W. Sijthoff.
- ROSE, J. E., BRUGGE, J. F., ANDERSON, D. J. & HIND, J. E. (1967). Phase-locked responses to low frequency tones in single auditory nerve fibres of the squirrel monkey. *J. Neurophysiol.* **30**, 769-793.
- ROSE, J. E., HIND, J. E., ANDERSON, D. J. & BRUGGE, J. F. (1971). Some effects of stimulus intensity on responses of auditory nerve fibres in the squirrel monkey. *J. Neurophysiol.* **34**, 685-699.
- RUSSELL, I. J. & SELICK, P. M. (1978). Intracellular studies of hair cells in the mammalian cochlea. *J. Physiol.* **284**, 261-290.
- SCHMIDT, R. S. & FERNÁNDEZ, C. (1962). Labyrinthine d.c. potentials in representative vertebrates. *J. cell. comp. Physiol.* **59**, 311-322.
- STEWART, W. W. (1978). Functional connections between cells as revealed by dye-coupling with a highly fluorescent naphthalimide tracer. *Cell*, **14**, 741-759.
- TER KUILE, E. (1900). Die Übertragung der Energie von der Grundmembran auf die Haarzellen. *Pflügers Arch. ges. Physiol.* **79**, 146-157.
- VON BÉKÉSY, G. (1960). *Experiments in Hearing*. New York & London: McGraw Hill.
- WALSH, B. T., MILLER, J. B., GACEK, R. R. & KIANG, N. Y. S. (1972). Spontaneous activity in the eighth cranial nerve of the cat. *Int. J. Neurosci.* **3**, 221-236.
- WEISS, T. F., MULROY, M. J., TURNER, R. G. & PIKE, C. L. (1976). Tuning of single fibres in the cochlear nerve of the alligator lizard: relation to receptor morphology. *Brain Res.* **115**, 71-90.





A. C. CRAWFORD AND R. FETTIPLACE



- WEISS, T. F., PEAKE, W. T., LING, A. & HOLTON, T. (1978). Which structures determine frequency selectivity and tonotopic organization of vertebrate cochlear nerve fibres? Evidence from the alligator lizard. In *Evoked Electrical Activity in the Auditory Nervous System*, eds. NAUNTON, R. F. & FERNÁNDEZ, C., pp. 91–112. New York, San Francisco & London: Academic Press.
- WEVER, E. G. (1971). The mechanics of hair cell stimulation. *Ann. Otol. Rhinol. Lar.* **80**, 786–804.
- WEVER, E. G. (1978). *The Reptile Ear: Its Structure and Function*. Princeton University Press.
- WEVER, E. G. & VERNON, J. R. (1956). Sound transmission in the turtle's ear. *Proc. natn. Acad. Sci. U.S.A.* **42**, 292–299.
- WIEDERHOLD, M. L. (1978). Membrane voltage noise associated with ciliary beating in the *Aplysia statocyst*. *Brain Res.* **156**, 369–374.

## EXPLANATION OF PLATES

## PLATE 1

Low power photomicrograph of a wholemount of the left cochlea of a juvenile *Pseudemys scripta elegans*. The cochlea has been lightly stained with Heidenhain's haematoxylin. The micrograph is focused at the plane of the hair cell nuclei in the basilar papilla (*bp*). The nerve fibres in the neural limb (*nl*) are also in focus as they dive anteriorly after leaving the papilla.

Other abbreviations: *a*, apical end of cochlea; *b*, basal end; *e*, abneural edge of basilar membrane; *l*, lagenar nerve; *p*, nerve to ampulla of posterior semicircular canal, nerve has been cut; VIII, auditory nerve. Calibration bar 100  $\mu\text{m}$ .

## PLATE 2

Photomicrographs of a transverse section of the basilar papilla to show localization of the electrode position by dye injection. *A*, fluorescence illumination showing a hair cell stained with Lucifer yellow. *B*, same section with Normarski optics. The histological preparation is described in the Methods; calibration bar 20  $\mu\text{m}$ , the magnification is the same in both micrographs. *tm*, tectorial membrane; *st*, scala tympani; *nl*, neural limb. Note that the dye has diffused into the cilia of the stained cell; ciliary bundles of other cells also visible in *B*.